

NUREG/CR-3723
ORNL/CSD/TM-216

MARTIN MARIETTA

Stress-Intensity-Factor Influence Coefficients for Surface Flaws in Pressure Vessels

D. G. Ball
B. R. Bass
J. W. Bryson
R. D. Cheverton
J. B. Drake

Prepared for the U.S. Nuclear Regulatory Commission
Office of Nuclear Regulatory Research
Under Interagency Agreements DOE 40-551-75 and 40-552-75

8503290280 850228
PDR NUREG
CR-3723 R PDR

OPERATED BY
MARTIN MARIETTA ENERGY SYSTEMS, INC.
FOR THE UNITED STATES
DEPARTMENT OF ENERGY

NOTICE

Availability of Reference Materials Cited in NRC Publications

Most documents cited in NRC publications will be available from one of the following sources:

1. The NRC Public Document Room, 1717 H Street, N.W., Washington, DC 20555
2. The NRC/GPO Sales Program, U.S. Nuclear Regulatory Commission, Washington, DC 20555
3. The National Technical Information Service, Springfield, VA 22161

Although the listing that follows represents the majority of documents cited in NRC publications, it is not intended to be exhaustive.

Referenced documents available for inspection and copying for a fee from the NRC Public Document Room include NRC correspondence and internal NRC memoranda; NRC Office of Inspection and Enforcement bulletins, circulars, information notices, inspection and investigation notices; Licensee Event Reports; vendor reports and correspondence; Commission papers; and applicant and licensee documents and correspondence.

The following documents in the NUREG series are available for purchase from the NRC/GPO Sales Program: formal NRC staff and contractor reports, NRC-sponsored conference proceedings, and NRC booklets and brochures. Also available are Regulatory Guides, NRC regulations in the *Code of Federal Regulations*, and *Nuclear Regulatory Commission Issuances*.

Documents available from the National Technical Information Service include NUREG series reports and technical reports prepared by other federal agencies and reports prepared by the Atomic Energy Commission, forerunner agency to the Nuclear Regulatory Commission.

Documents available from public and special technical libraries include all open literature items, such as books, journal and periodical articles, and transactions. *Federal Register* notices, federal and state legislation, and congressional reports can usually be obtained from these libraries.

Documents such as theses, dissertations, foreign reports and translations, and non-NRC conference proceedings are available for purchase from the organization sponsoring the publication cited.

Single copies of NRC draft reports are available free, to the extent of supply, upon written request to the Division of Technical Information and Document Control, U.S. Nuclear Regulatory Commission, Washington, DC 20555.

Copies of industry codes and standards used in a substantive manner in the NRC regulatory process are maintained at the NRC Library, 7920 Norfolk Avenue, Bethesda, Maryland, and are available there for reference use by the public. Codes and standards are usually copyrighted and may be purchased from the originating organization or, if they are American National Standards, from the American National Standards Institute, 1430 Broadway, New York, NY 10018.

Notice

This report was prepared as an account of work sponsored by an agency of the United States Government. Neither the United States Government nor any agency thereof, nor any of their employees, makes any warranty, express or implied, or assumes any legal liability or responsibility for the accuracy, completeness, or usefulness of any information, apparatus, product, or process disclosed, or represents that its use would not infringe privately owned rights. Reference herein to any specific commercial product, process, or service by trade name, trademark, manufacturer, or otherwise, does not necessarily constitute or imply its endorsement, recommendation, or favoring by the United States Government or any agency thereof. The views and opinions of authors expressed herein do not necessarily state or reflect those of the United States Government or any agency thereof.

NUREG/CR-3723
ORNL/CSD/TM-216
Dist. Category RF

Engineering Technology Division

STRESS-INTENSITY-FACTOR INFLUENCE COEFFICIENTS
FOR SURFACE FLAWS IN PRESSURE VESSELS

D. G. Ball* J. W. Bryson
B. R. Bass* R. D. Cheverton
 J. B. Drake*

*Computing and Telecommunications Division

Manuscript Completed - January 11, 1985
Date of Issue - February 1985

NOTICE: This document contains information of a preliminary nature. It is subject to revision or correction and therefore does not represent a final report.

Prepared for the
U.S. Nuclear Regulatory Commission
Office of Nuclear Regulatory Research
Washington, DC 20555
under Interagency Agreements DOE 40-551-75 and 40-552-75

NRC FIN No. B0119

Prepared by the
OAK RIDGE NATIONAL LABORATORY
Oak Ridge, Tennessee 37831
operated by
MARTIN MARIETTA ENERGY SYSTEMS, INC.
for the
U.S. DEPARTMENT OF ENERGY
under Contract No. DE-AC05-84OR21400

CONTENTS

	<u>Page</u>
LIST OF FIGURES	v
LIST OF TABLES	vii
FOREWORD	ix
ABSTRACT	i
1. INTRODUCTION	1
2. SUPERPOSITION AND INFLUENCE COEFFICIENTS	3
3. CALCULATION AND EVALUATION OF INFLUENCE COEFFICIENTS FOR SPECIFIC 3-D FLAWS	8
3.1 Computer Codes	8
3.2 Mesh Design	8
3.3 Mesh Convergence Studies	8
3.4 90° vs 180° Model	11
3.5 Length of Cylinder	13
3.6 Adequacy of Third-Order Polynomial to Represent Stress Distribution	13
3.7 Accommodation of Cladding	17
4. COMPARISONS WITH OTHER INVESTIGATORS	19
5. INFLUENCE COEFFICIENTS FOR SPECIFIC APPLICATIONS	22
5.1 Pressurized Water Reactor	22
5.2 Pressurized-Thermal-Shock-Experiment Test Vessel	22
REFERENCES	24
APPENDIX A. INFLUENCE COEFFICIENTS FOR THE 2-m FLAW IN A PWR ...	27
APPENDIX B. INFLUENCE COEFFICIENTS FOR THE 6/1 FLAW IN A PWR ...	33
APPENDIX C. INFLUENCE COEFFICIENTS FOR THE 1-m FLAW IN A PTSE VESSEL	35

LIST OF FIGURES

<u>Figure</u>		<u>Page</u>
2.1	Graphical representation of method for calculating K_I using equivalent problem	4
2.2	Method of calculating K_I using superposition principle	5
2.3	Axially oriented semielliptical flaw on inner surface of cylinder	6
2.4	Crack-surface loading cases for determining 3-D flaw influence coefficients	7
3.1	Sample mesh in crack plane for $a/w = 0.2$, $c/a = 2.5$	9
3.2	Sample mesh viewed from axial direction	10
3.3	90° and 180° models used for determining difference in K_I values for single axial flaw and two opposite flaws	11
3.4	Thermal stress profile in PWR used for comparison calculation of K_I in Table 3.1	12
3.5	Thermal stress profile in PWR used to calculate K_I given in Fig. 3.6	14
3.6	Comparison of K_I values calculated by superposition and direct FE techniques for axially oriented, inner-surface 2-m flaw ($a/w = 0.6$) in PWR vessel during severe thermal transient	15
3.7	Thermal stress profile in PTSE test vessel used to calculate K_I given in Fig. 3.8	16
3.8	Comparison of 3-D superposition with 3-D direct analysis for axially oriented, outer-surface 1-m flaw in PTSE test vessel	17
3.9	Stress distributions used in superposition techniques for including effect of cladding on K_I	18
4.1	Influence coefficients for longitudinal semielliptical crack on inner surface of cylinder: $a/w = 0.2$, $c/a = 2.5$, $R_0/R_1 = 1.1$	19
4.2	Influence coefficients for longitudinal semielliptical crack on inner surface of cylinder: $a/w = 0.5$, $c/a = 2.5$, $R_0/R_1 = 1.1$	20
4.3	Influence coefficients for longitudinal semielliptical crack on inner surface of cylinder: $a/w = 0.8$, $c/a = 3$, $R_0/R_1 = 1.1$	20

<u>Figure</u>		<u>Page</u>
5.1	PTSE test vessel with longitudinal outer-surface crack	23
A.1	Influence coefficients for 2-m flaw at $\phi = 90^\circ$	30
A.2	Cladding influence coefficients for 2-m flaw at $\phi = 90^\circ$	31
B.1	Influence coefficients for 6/1 flaw at $\phi = 90^\circ$	34
C.1	Influence coefficients for 1-m outer-surface flaw at deepest point ($\phi = 90^\circ$)	35

LIST OF TABLES

<u>Table</u>		<u>Page</u>
3.1	Comparison of K_I values for 2-D flaws in 90° and 180° models	12
A.1	Influence coefficients for the 2-m flaw in a PWR	28
B.1	Influence coefficients for the 6/1 flaw in a PWR	33
C.1	Influence coefficients for the 1-m flaw in a PTSE test vessel	36

FOREWORD

The work reported here was performed at Oak Ridge National Laboratory (ORNL) under the Heavy-Section Steel Technology (HSST) Program, C. E. Pugh, Program Manager. The program is sponsored by the Office of Nuclear Regulatory Research of the U.S. Nuclear Regulatory Commission (NRC). The technical monitor for the NRC is Milton Vagins.

This report is designated HSST Program Technical Report 77. Prior reports in this series are listed below:

1. S. Yukawa, *Evaluation of Periodic Proof Testing and Warm Prestressing Procedures for Nuclear Reactor Vessels*, HSSTP-TR-1, General Electric Company, Schenectady, N. Y. (July 1, 1969).
2. L. W. Loechel, *The Effect of Testing Variables on the Transition Temperature in Steel*, MCR-69-189, Martin Marietta Corporation, Denver, Colo. (November 20, 1969).
3. P. N. Randall, *Gross Strain Measure of Fracture Toughness of Steels*, HSSTP-TR-3, TRW Systems Group, Redondo Beach, Calif. (November 1, 1969).
4. C. Visser, S. E. Gabrielse, and W. VanBuren, *A Two-Dimensional Elastic-Plastic Analysis of Fracture Test Specimens*, WCAP-7368, Westinghouse Electric Corporation, PWR Systems Division, Pittsburgh, Pa. (October 1969).
5. T. R. Mager and F. O. Thomas, *Evaluation by Linear Elastic Fracture Mechanics of Radiation Damage to Pressure Vessel Steels*, WCAP-7328 (Rev.), Westinghouse Electric Corporation, PWR Systems Division, Pittsburgh, Pa. (October 1969).
6. W. O. Shabbits, W. H. Pryle, and E. W. Wessel, *Heavy-Section Fracture Toughness Properties of A533 Grade B Class 1 Steel Plate and Submerged Arc Weldment*, WCAP-7414, Westinghouse Electric Corporation, PWR Systems Division, Pittsburgh, Pa. (December 1969).
7. F. J. Loss, *Dynamic Tear Test Investigations of the Fracture Toughness of Thick-Section Steel*, NRL-7056, Naval Research Laboratory, Washington, D.C. (May 14, 1970).
8. P. B. Crosley and E. J. Ripling, *Crack Arrest Fracture Toughness of A533 Grade B Class 1 Pressure Vessel Steel*, HSSTP-TR-8, Materials Research Laboratory, Inc., Glenwood, Ill. (March 1970).
9. T. R. Mager, *Post-Irradiation Testing of 2T Compact Tension Specimens*, WCAP-7561, Westinghouse Electric Corporation, PWR Systems Division, Pittsburgh, Pa. (August 1970).
10. T. R. Mager, *Fracture Toughness Characterization Study of A533, Grade B, Class 1 Steel*, WCAP-7578, Westinghouse Electric Corporation, PWR Systems Division, Pittsburgh, Pa. (October 1970).

11. T. R. Mager, *Notch Preparation in Compact Tension Specimens*, WCAP-7579, Westinghouse Electric Corporation, PWR Systems Division, Pittsburgh, Pa. (November 1970).
12. N. Levy and P. V. Marcal, *Three-Dimensional Elastic-Plastic Stress and Strain Analysis for Fracture Mechanics, Phase I: Simple Flawed Specimens*, HSSTP-TR-12, Brown University, Providence, R.I. (December 1970).
13. W. O. Shabbits, *Dynamic Fracture Toughness Properties of Heavy Section A533 Grade B Class 1 Steel Plate*, WCAP-7623, Westinghouse Electric Corporation, PWR Systems Division, Pittsburgh, Pa. (December 1970).
14. P. N. Randall, *Gross Strain Crack Tolerance of A533-B Steel*, HSSTP-TR-14, TRW Systems Group, Redondo Beach, Calif. (May 1, 1971).
15. H. T. Corten and R. H. Sailors, *Relationship Between Material Fracture Toughness Using Fracture Mechanics and Transition Temperature Tests*, T&AM Report 346, University of Illinois, Urbana, Ill. (August 1, 1971).
16. T. R. Mager and V. J. McLoughlin, *The Effect of an Environment of High Temperature Primary Grade Nuclear Reactor Water on the Fatigue Crack Growth Characteristics of A533 Grade B Class 1 Plate and Weldment Material*, WCAP-7776, Westinghouse Electric Corporation, PWR Systems Division, Pittsburgh, Pa. (October 1971).
17. N. Levy and P. V. Marcal, *Three-Dimensional Elastic-Plastic Stress and Strain Analysis for Fracture Mechanics, Phase II: Improved Modelling*, HSSTP-TR-17, Brown University, Providence, R.I. (November 1971).
18. S. C. Grigory, *Tests of 6-in.-Thick Flawed Tensile Specimens, First Technical Summary Report, Longitudinal Specimens Numbers 1 through 7*, HSSTP-TR-18, Southwest Research Institute, San Antonio, Tex. (June 1972).
19. P. N. Randall, *Effects of Strain Gradients on the Gross Strain Crack Tolerance of A533-B Steel*, HSSTP-TR-19, TRW Systems Group, Redondo Beach, Calif. (June 15, 1972).
20. S. C. Grigory, *Tests of 6-Inch-Thick Flawed Tensile Specimens, Second Technical Summary Report, Transverse Specimens Numbers 8 through 10, Welded Specimens Numbers 11 through 13*, HSSTP-TR-20, Southwest Research Institute, San Antonio, Tex. (June 1972).
21. L. A. James and J. A. Williams, *Heavy Section Steel Technology Program Technical Report No. 21, The Effect of Temperature and Neutron Irradiation Upon the Fatigue-Crack Propagation Behavior of ASTM A533 Grade B, Class 1 Steel*, HEDL-TME 72-132, Hanford Engineering Development Laboratory, Richland, Wash. (September 1972).

22. S. C. Grigory, *Tests of 6-Inch-Thick Flawed Tensile Specimens, Third Technical Summary Report, Longitudinal Specimens Numbers 14 through 16, Unflawed Specimen Number 17*, HSSTP-TR-22, Southwest Research Institute, San Antonio, Tex. (October 1972).
23. S. C. Grigory, *Tests of 6-Inch Thick Tensile Specimens, Fourth Technical Summary Report, Tests of 1-Inch-Thick Flawed Tensile Specimens for Size Effect Evaluation*, HSSTP-TR-23, Southwest Research Institute, San Antonio, Tex. (June 1973).
24. S. P. Ying and S. C. Grigory, *Tests of 6-Inch-Thick Tensile Specimens, Fifth Technical Summary Report, Acoustic Emission Monitoring of One-Inch and Six-Inch-Thick Tensile Specimens*, HSSTP-TR-24, Southwest Research Institute, San Antonio, Tex. (November 1972).
25. R. W. Derby, J. G. Merkle, G. C. Robinson, G. D. Whitman, and F. J. Witt, *Test of 6-Inch-Thick Pressure Vessels. Series 1: Intermediate Test Vessels V-1 and V-2*, ORNL-4895, Oak Ridge Natl. Lab., Oak Ridge, Tenn. (February 1974).
26. W. J. Stelzman and R. G. Berggren, *Radiation Strengthening and Embrittlement in Heavy Section Steel Plates and Welds*, ORNL-4871, Oak Ridge Natl. Lab., Oak Ridge, Tenn. (June 1973).
27. P. B. Crosley and E. J. Ripling, *Crack Arrest in an Increasing K-Field*, HSSTP-TR-27, Materials Research Laboratory, Inc., Glenwood, Ill. (January 1973).
28. P. V. Marcal, P. M. Stuart, and R. S. Bettles, *Elastic-Plastic Behavior of a Longitudinal Semi-Elliptic Crack in a Thick Pressure Vessel*, HSSTP-TR-28, Brown University, Providence, R.I. (June 1973).
29. W. J. Stelzman, R. G. Berggren, and T. N. Jones, *ORNL Characterization of Heavy-Section Steel Technology Program Plates 01, 02 and 03 (in preparation)*.
30. Canceled.
31. J. A. Williams, *The Irradiation and Temperature Dependence of Tensile and Fracture Properties of ASTM A533, Grade B, Class 1 Steel Plate and Weldment*, HEDL-TME 73-75, Hanford Engineering Development Laboratory, Richland, Wash. (August 1973).
32. J. M. Steichen and J. A. Williams, *High Strain Rate Tensile Properties of Irradiated ASTM A533 Grade B Class 1 Pressure Vessel Steel*, Hanford Engineering Development Laboratory, Richland, Wash. (July 1973).
33. P. C. Riccardella and J. L. Swedlow, *A Combined Analytical-Experimental Fracture Study of the Two Leading Theories of Elastic-Plastic Fracture (J-Integral and Equivalent Energy)*, WCAP-8224, Westinghouse Electric Corporation, Pittsburgh, Pa. (October 1973).
34. R. J. Podlasek and R. J. Eiber, *Final Report on Investigation of Mode III Crack Extension in Reactor Piping*, Battelle Columbus Laboratories, Columbus, Ohio (December 14, 1973).

35. T. R. Mager, J. D. Landes, D. M. Moon, and V. J. McLaughlin, *Interim Report on the Effect of Low Frequencies on the Fatigue Crack Growth Characteristics of A533 Grade B Class 1 Plate in an Environment of High-Temperature Primary Grade Nuclear Reactor Water*, WCAP-8256, Westinghouse Electric Corporation, Pittsburgh, Pa. (December 1973).
36. J. A. Williams, *The Irradiated Fracture Toughness of ASTM A533, Grade B, Class 1 Steel Measured with a Four-Inch-Thick Compact Tension Specimen*, HEDL-TME 75-10, Hanford Engineering Development Laboratory, Richland, Wash. (January 1975).
37. R. H. Bryan, J. G. Merkle, M. N. Raftenberg, G. C. Robinson, and J. E. Smith, *Test of 6-Inch-Thick Pressure Vessels. Series 2: Intermediate Test Vessels V-3, V-4, and V-6*, ORNL-5059, Oak Ridge Natl. Lab., Oak Ridge, Tenn. (November 1975).
38. T. R. Mager, S. E. Yanichko, and L. R. Singer, *Fracture Toughness Characterization of HSST Intermediate Pressure Vessel Material*, WCAP-8456, Westinghouse Electric Corporation, Pittsburgh, Pa. (December 1974).
39. J. G. Merkle, G. D. Whitman, and R. H. Bryan, *An Evaluation of the HSST Program Intermediate Pressure Vessel Tests in Terms of Light-Water-Reactor Pressure Vessel Safety*, ORNL/TM-5090, Oak Ridge Natl. Lab., Oak Ridge, Tenn. (November 1975).
40. J. G. Merkle, G. C. Robinson, P. P. Holz, J. E. Smith, and R. H. Bryan, *Test of 6-In.-Thick Pressure Vessels. Series 3: Intermediate Test Vessel V-7*, ORNL/NUREG-1, Oak Ridge Natl. Lab., Oak Ridge, Tenn. (August 1976).
41. J. A. Davidson, L. J. Ceschini, R. P. Shogan, and G. V. Rao, *The Irradiated Dynamic Fracture Toughness of ASTM A533, Grade B, Class 1 Steel Plate and Submerged Arc Weldment*, WCAP-8775, Westinghouse Electric Corporation, Pittsburgh, Pa. (October 1976).
42. R. D. Cheverton, *Pressure Vessel Fracture Studies Pertaining to PWR LOCA-ECC Thermal Shock: Experiments TSE-1 and TSE-2*, ORNL/NUREG/TM-31, Oak Ridge Natl. Lab., Oak Ridge, Tenn. (September 1976).
43. J. G. Merkle, G. C. Robinson, P. P. Holz, and J. E. Smith, *Test of 6-In.-Thick Pressure Vessels. Series 4: Intermediate Test Vessels V-5 and V-9 with Inside Nozzle Corner Cracks*, ORNL/NUREG-7, Oak Ridge Natl. Lab., Oak Ridge, Tenn. (August 1977).
44. J. A. Williams, *The Ductile Fracture Toughness of Heavy Section Steel Plate*, Hanford Engineering Development Laboratory, Richland, Wash., NUREG/CR-0859 (September 1979).
45. R. H. Bryan, T. M. Cate, P. P. Holz, T. A. King, J. G. Merkle, G. C. Robinson, G. C. Smith, J. E. Smith, and G. D. Whitman, *Test of 6-in.-Thick Pressure Vessels. Series 3: Intermediate Test Vessel V-7A Under Sustained Loading*, ORNL/NUREG-9, Oak Ridge Natl. Lab., Oak Ridge, Tenn. (February 1978).

46. R. D. Cheverton and S. E. Bolt, *Pressure Vessel Fracture Studies Pertaining to a PWR LOCA-ECC Thermal Shock: Experiments TSE-3 and TSE-4 and Update of TSE-1 and TSE-2 Analysis*, ORNL/NUREG-22, Oak Ridge Natl. Lab., Oak Ridge, Tenn. (December 1977).
47. D. A. Canonico, *Significance of Reheat Cracks to the Integrity of Pressure Vessels for Light-Water Reactors*, ORNL/NUREG-15, Oak Ridge Natl. Lab., Oak Ridge, Tenn. (July 1977).
48. G. C. Smith and P. P. Holz, *Repair Weld Induced Residual Stresses in Thick-Walled Steel Pressure Vessels*, NUREG/CR-0093 (ORNL/NUREG/TM-153), Oak Ridge Natl. Lab., Oak Ridge, Tenn. (June 1978).
49. P. P. Holz and S. W. Wismer, *Half-Bead (Temper) Repair Welding for HSST Vessels*, NUREG/CR-0113 (ORNL/NUREG/TM-177), Oak Ridge Natl. Lab., Oak Ridge, Tenn. (June 1978).
50. G. C. Smith, P. P. Holz, and W. J. Stelzman, *Crack Extension and Arrest Tests of Axially Flawed Steel Model Pressure Vessels*, NUREG/CR-0126 (ORNL/NUREG/TM-196), Oak Ridge Natl. Lab., Oak Ridge, Tenn. (October 1978).
51. R. H. Bryan, P. P. Holz, J. G. Merkle, G. C. Smith, J. E. Smith, and W. J. Stelzman, *Test of 6-in.-Thick Pressure Vessels. Series 3: Intermediate Test Vessel V-7B*, NUREG/CR-0309 (ORNL/NUREG-38), Oak Ridge Natl. Lab., Oak Ridge, Tenn. (October 1978).
52. R. D. Cheverton, S. K. Iskander, and S. E. Bolt, *Applicability of LEFM to the Analysis of PWR Vessels Under LOCA-ECC Thermal Shock Conditions*, NUREG/CR-0107 (ORNL/NUREG-40), Oak Ridge Natl. Lab., Oak Ridge, Tenn. (October 1978).
53. R. H. Bryan, D. A. Canonico, P. P. Holz, S. K. Iskander, J. G. Merkle, J. E. Smith, and W. J. Stelzman, *Test of 6-in.-Thick Pressure Vessels, Series 3: Intermediate Test Vessel V-8*, NUREG/CR-0675 (ORNL/NUREG-58), Oak Ridge Natl. Lab., Oak Ridge, Tenn. (December 1979).
54. R. D. Cheverton and S. K. Iskander, *Application of Static and Dynamic Crack Arrest Theory to TSE-4*, NUREG/CR-0767 (ORNL/NUREG-57), Oak Ridge Natl. Lab., Oak Ridge, Tenn. (June 1979).
55. J. A. Williams, *Tensile Properties of Irradiated and Unirradiated Welds of A533 Steel Plate and A508 Forgings*, NUREG/CR-1158 (ORNL/Sub-79/50917/2), Hanford Engineering Development Laboratory, Richland, Wash. (July 1979).
56. K. W. Carlson and J. A. Williams, *The Effect of Crack Length and Side Grooves on the Ductile Fracture Toughness Properties of ASTM A533 Steel*, NUREG/CR-1171 (ORNL/Sub-79/50917/3), Hanford Engineering Development Laboratory, Richland, Wash. (October 1979).
57. P. P. Holz, *Flaw Preparations for HSST Program Vessel Fracture Mechanics Testing; Mechanical-Cyclic Pumping and Electron-Beam Weld-Hydrogen Charge Cracking Schemes*, NUREG/CR-1274 (ORNL/NUREG/TM-369), Oak Ridge Natl. Lab., Oak Ridge, Tenn. (May 1980).

58. S. K. Iskander, *Two Finite Element Techniques for Computing Mode I Stress Intensity Factors in Two- or Three-Dimensional Problems*, NUREG/CR-1499 (ORNL/NUREG/CSD/TM-14), Computer Sciences Div., Union Carbide Corp. Nuclear Div., Oak Ridge, Tenn. (February 1981).
59. P. B. Crosley and E. J. Ripling, *Development of a Standard Test for Measuring K_{Ia} with a Modified Compact Specimen*, NUREG/CR-2294 (ORNL/Sub-81/7755/1), Materials Research Laboratory, Glenwood, Ill. (August 1981).
60. S. N. Atluri, B. R. Bass, J. W. Bryson, and K. Kathiresan, *NOZ-FLAW: A Finite Element Program for Direct Evaluation of Stress Intensity Factors for Pressure Vessel Nozzle-Corner Flaws*, NUREG/CR-1843, (ORNL/NUREG/CSD/TM-18), Computer Sciences Div., Oak Ridge Gaseous Diffusion Plant, Oak Ridge, Tenn. (March 1981).
61. A. Shukla, W. L. Fourney, and G. R. Irwin, *Study of Energy Loss and Its Mechanisms in Homalite 100 During Crack Propagation and Arrest*, NUREG/CR-2150 (ORNL/Sub-7778/1), University of Maryland, College Park, Md. (August 1981).
62. S. K. Iskander, R. D. Cheverton, and D. G. Ball, *OCA-1, A Code for Calculating the Behavior of Flaws on the Inner Surface of a Pressure Vessel Subjected to Temperature and Pressure Transients*, NUREG/CR-2113 (ORNL/NUREG-84), Oak Ridge Natl. Lab., Oak Ridge, Tenn. (August 1981).
63. R. J. Sanford, R. Chona, W. L. Fourney, and G. R. Irwin, *A Photo-elastic Study of the Influence of Non-Singular Stresses in Fracture Test Specimens*, NUREG/CR-2179 (ORNL/Sub-7778/2), University of Maryland, College Park, Md. (August 1981).
64. B. R. Bass, S. N. Atluri, J. W. Bryson, and K. Kathiresan, *OR-FLAW: A Finite Element Program for Direct Evaluation of K-Factors for User-Defined Flaws in Plate, Cylinders, and Pressure-Vessel Nozzle Corners*, NUREG/CR-2494 (ORNL/CSD/TM-165) (April 1982).
65. B. R. Bass and J. W. Bryson, *ORMGEN-3D: A Finite Element Mesh Generator for 3-Dimensional Crack Geometries*, NUREG/CR-2997, Vol. 1 (ORNL/TM-8527/V1), Oak Ridge Natl. Lab., Oak Ridge, Tenn. (December 1982).
66. B. R. Bass and J. W. Bryson, *ORVIRT: A Finite Element Program for Energy Release Rate Calculations for 2-Dimensional and 3-Dimensional Crack Models*, NUREG/CR-2997, Vol. 2 (ORNL/TM-8527/V2), Oak Ridge Natl. Lab., Oak Ridge, Tenn. (February 1983).
67. R. D. Cheverton, S. K. Iskander, and D. G. Ball, *PWR Pressure Vessel Integrity During Overcooling Accidents: A Parametric Analysis*, NUREG/CR-2895 (ORNL/TM-7931), Oak Ridge Natl. Lab., Oak Ridge, Tenn. (February 1983).
68. D. G. Ball, R. D. Cheverton, J. B. Drake, and S. K. Iskander, *OCA-II, A Code for Calculating Behavior of 2-D and 3-D Surface Flaws in a Pressure Vessel Subjected to Temperature and Pressure Transients*, NUREG/CR-3491 (ORNL-5934), Oak Ridge Natl. Lab., Oak Ridge, Tenn. (February 1984).

69. A. Sauter, R. D. Cheverton, and S. K. Iskander, *Modification of OCA-I for Application to a Reactor Pressure Vessel with Cladding on the Inner Surface*, NUREG/CR-3155 (ORNL/TM-8649), Oak Ridge Natl. Lab., Oak Ridge, Tenn. (May 1983).
70. R. D. Cheverton and D. G. Ball, *OCA-P, A Deterministic and Probabilistic Fracture-Mechanics Code for Application to Pressure Vessels*, NUREG/CR-3618 (ORNL-5991), Oak Ridge Natl. Lab., Oak Ridge, Tenn. (May 1984).
71. J. G. Merkle, *An Examination of the Size Effects and Data Scatter Observed in Small Specimen Cleavage Fracture Toughness Testing*, NUREG/CR-3672 (ORNL/TM-9088), Oak Ridge Natl. Lab., Oak Ridge, Tenn. (April 1984).
72. C. E. Pugh et al., *Heavy-Section Steel Technology Program — Five-Year Plan FY 1983-1987*, NUREG/CR-3595 (ORNL/TM-9008), Oak Ridge Natl. Lab., Oak Ridge, Tenn. (April 1984).

STRESS-INTENSITY-FACTOR INFLUENCE COEFFICIENTS FOR
SURFACE FLAWS IN PRESSURE VESSELS

D. G. Ball* J. W. Bryson
B. R. Bass* R. D. Cheverton
J. B. Drake*

ABSTRACT

In the fracture-mechanics analysis of reactor pressure vessels, stress-intensity-factor influence coefficients are used in conjunction with superposition techniques to reduce the cost of calculating stress-intensity factors. The present study uses a finite-element code, together with a virtual crack extension technique, to obtain influence coefficients for semielliptical surface flaws in a cylinder, and particular emphasis was placed on mesh convergence (less than 1% error was sought in the results from any one mesh construction parameter). Comparison of the coefficients with those obtained by other investigators shows good agreement. Furthermore, stress-intensity factors obtained by superposition for a severe thermal-transient loading condition agree within 1% of the values calculated by a direct finite-element method.

Influence coefficients were calculated for three specific axially oriented semielliptical surface flaws. The first was a 2-m-long inner-surface flaw in a nuclear reactor pressure vessel with depth-to-wall-thickness ratios between 0.2 and 0.9. The second was an inner-surface flaw in the reactor vessel with a surface-length-to-depth ratio of 6 and with depth-to-wall-thickness ratios between 0.05 and 0.2. The third was a 1-m-long flaw on the outer surface of a test vessel with depth-to-wall-thickness ratios between 0.1 and 0.9. For the reactor vessel, separate coefficients were calculated for the cladding on the inner surface and for the base-material region. This allows for an accurate accounting of the effect of thermal stresses in the cladding on the stress-intensity factor for surface flaws that extend through the cladding into the base material.

1. INTRODUCTION

An evaluation of pressurized-water reactor (PWR) pressure-vessel integrity during postulated overcooling accidents¹ requires the application

*Computing and Telecommunications Division.

of linear-elastic fracture mechanics (LEFM). This involves the calculation of stress-intensity factors (K_I) for both two-dimensional (2-D) and three-dimensional (3-D) surface flaws subjected to combined thermal and pressure loadings. Under these circumstances, a sufficiently accurate determination of K_I requires the use of finite-element (FE) analysis, an approach that has been developed and applied by numerous investigators (for examples see Refs. 2-6). However, computer costs for the direct FE analysis of cracks can be prohibitive when a large number of calculations must be made, as is the case for parametric, reactor transient, and probabilistic studies.

In the last several years, an alternative approach to the direct FE method has been promoted that makes use of superposition techniques and stress-intensity-factor influence coefficients⁷⁻¹² that correspond to simple basic load distributions on the crack face. The coefficients must be obtained from FE analyses of specific structures and flaws of interest; however, once available, the coefficients can be weighted by any actual crack-free stress distribution normal to the plane of the crack face and summed to obtain the total K_I value. Because only the predetermined influence coefficients and the crack-free stress distributions are necessary to calculate K_I , this alternative approach is particularly suitable for parametric studies of a specific PWR pressure vessel.

In this report, the use of influence coefficients with superposition techniques is described; mesh-convergence studies conducted to ensure reasonable accuracy for the influence coefficients are discussed; K_I values obtained by superposition for severe thermal-shock loading conditions are compared with values calculated with the direct FE method; coefficients are compared with those obtained by other investigators; and influence coefficients are calculated for three specific axially oriented, semielliptical surface flaws in a cylinder. Two of these flaws are on the inner surface of a PWR reactor pressure vessel, and the other is on the outer surface of a test vessel. One of the reactor vessel flaws has a length of 1.8 m (referred to as the 2-m flaw), while the other has a surface-length-to-depth ratio of 6 (6/1 flaw). The test vessel flaw has a surface length of 1.0 m (1-m flaw).

2. SUPERPOSITION AND INFLUENCE COEFFICIENTS

The superposition technique, used in conjunction with the influence coefficients, makes use of the stresses in the uncracked structure, and, as discussed in Ref. 11 and illustrated in Fig. 2.1, only that portion of the stress distribution corresponding to the location of the crack face needs to be used. For an arbitrary stress distribution, such as that shown in Fig. 2.1, and for the case of a 2-D (long) flaw, the K_I value corresponding to the truncated stress distribution can be obtained by dividing the distribution into a reasonable number of equivalent forces on the crack face and then adding the K_I values corresponding to each of the forces. For convenience, normalized K_I values can be calculated for a number of individual unit loads along the crack face for all crack depths of interest (Fig. 2.2). These normalized K_I values, referred to as K_I^* and/or influence coefficients in these studies, can be weighted by any truncated stress distribution and added to obtain the total K_I value as indicated by Eq. (1).

$$K_I(a) = \sum_{i=1}^n \sigma_i \Delta a_i K_I^*(a_i', a), \quad (1)$$

where

Δa_i = an increment of about a' ,

$$\sum_{i=1}^n \Delta a_i = a,$$

a_i' = radial distance from open end of crack (cylinder surface) to point of application of unit load,

σ_i = average stress over Δa_i for equivalent problem,

K_I^* = stress-intensity factor per unit load applied at a_i' per unit length of cylinder,

n = number of points along length of crack for which K^* values are available.

The K_I^* values are dependent on the nature of the structure in which the cracks reside. However, for a given structure, the same set of K_I^* values can be used for any stress distribution provided there are enough K_I^* values along the face of the crack to adequately represent the stress distribution. As indicated in Ref. 12, the authors have used no less than 6 K_I^* values for very shallow inner-surface flaws in thick-walled cylinders, and as many as 46 for deep flaws (these K_I^* values were calculated using the FE code FMECH³).

ORNL-DWG 81-8076 ETD

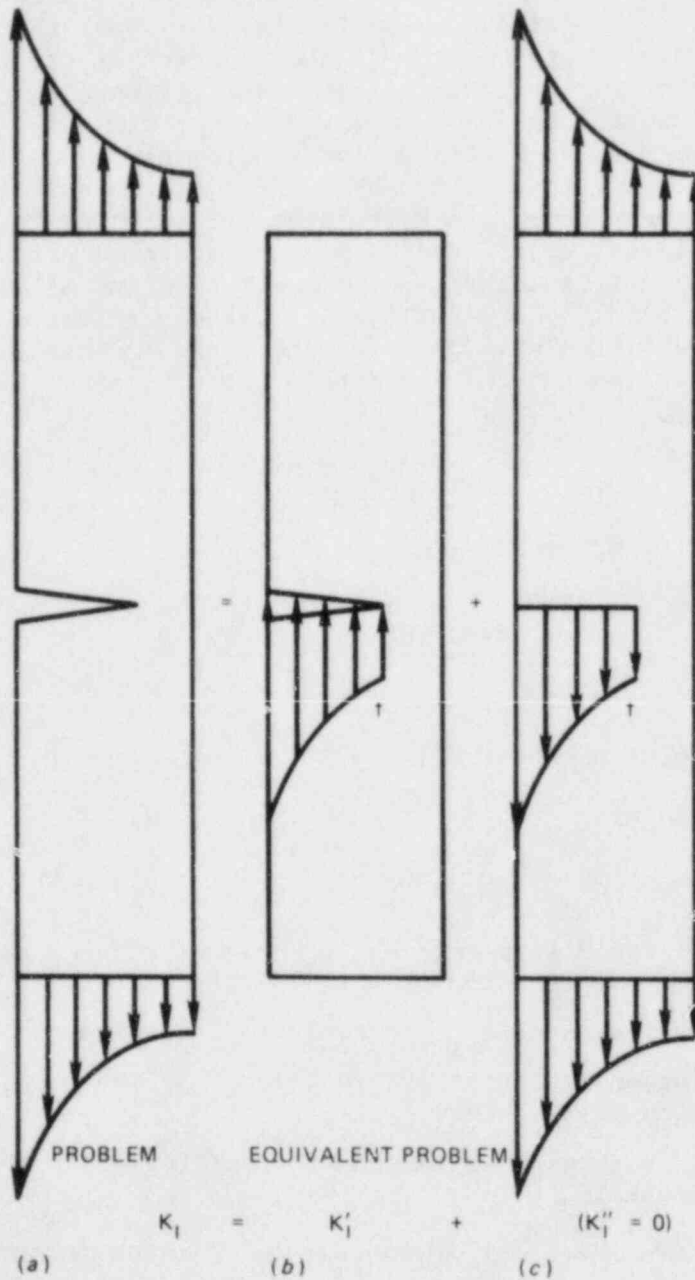
↑ FORCES SHOWN APPLIED TO UPPER SURFACE, OPPOSITE
IN SIGN APPLIED TO LOWER SURFACE

Fig. 2.1. Graphical representation of method for calculating K_I using equivalent problem.

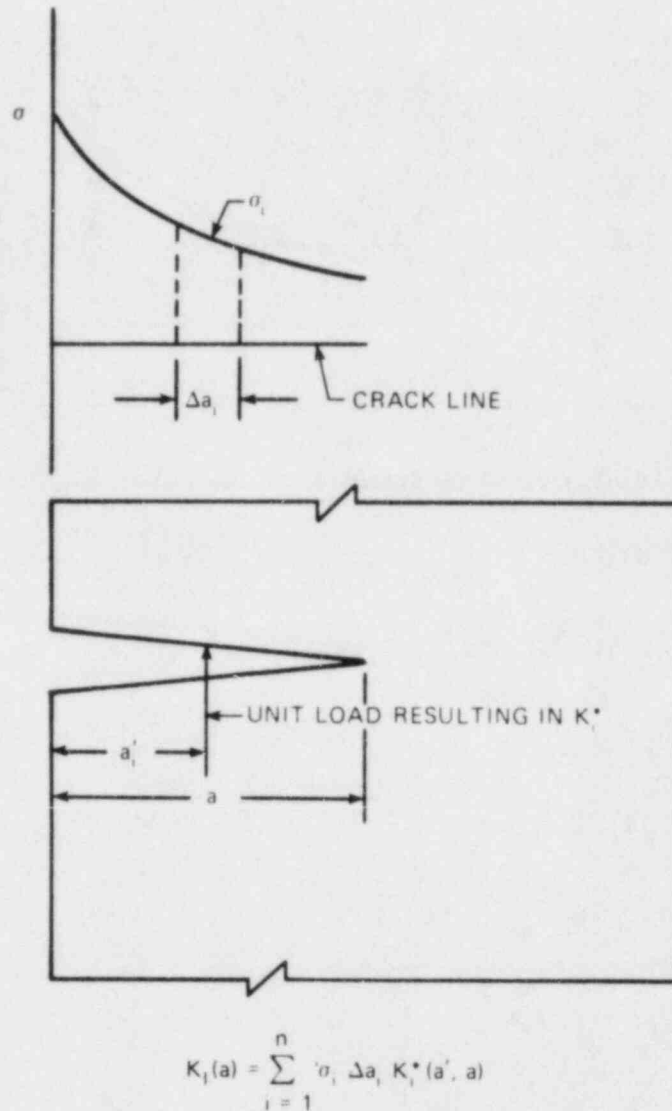


Fig. 2.2. Method of calculating K_I using superposition principle.

The influence coefficients for 3-D flaws are obtained in a somewhat different manner. For these flaws, the truncated stress distribution is approximated with a polynomial as indicated by Eq. (2):

$$\sigma(a') = C_0 + C_1 \left(\frac{a'}{a}\right) + C_2 \left(\frac{a'}{a}\right)^2 + C_3 \left(\frac{a'}{a}\right)^3, \quad (2)$$

where $\sigma(a')$ is the stress normal to the crack plane at radial position a' , and a' and a are defined in Fig. 2.3. The K_I values are calculated for each of the individual terms (stress distributions) in Eq. (2) and

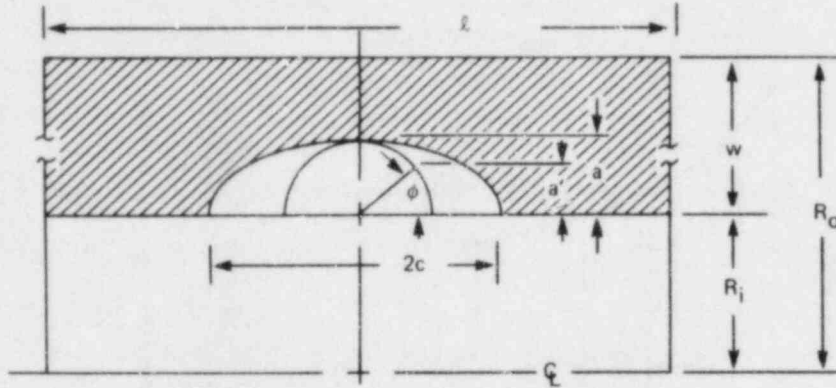


Fig. 2.3. Axially oriented semielliptical flaw on inner surface of cylinder.

are then added to obtain the total K_I value as indicated by Eq. (3):

$$K_I(a) = \sum_{j=0}^3 K_{Ij}(a) = \sum_{j=0}^3 C_j \sqrt{\pi a} K_j^*(a), \quad (3)$$

where

$$K_j^*(a) = K_{Ij}'(a) / (C_j' \sqrt{\pi a}). \quad (4)$$

Values of $K_{Ij}'(a)/C_j'$ are calculated for each of the normalized stress distributions corresponding to each term in Eq. (2) (see Fig. 2.4), using a 3-D finite-element analysis and an arbitrary value of C_j' , such as unity. The quantity $K_j^*(a)$ is referred to as the influence coefficient and, as indicated by Eq. (4), is dimensionless. Once the influence coefficients are obtained, they can be used with any values of C_j to obtain corresponding values of $K_I(a)$.

For 3-D flaws, $K_j^*(a)$ values can be calculated for several points along the crack front, in which case Eq. (3) becomes

$$K_I(\phi) = \sum_{j=0}^3 C_j \sqrt{\pi a} K_j^*(\phi), \quad (5)$$

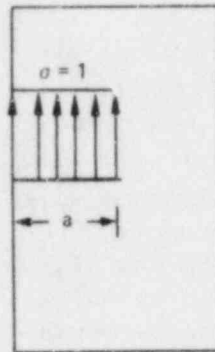
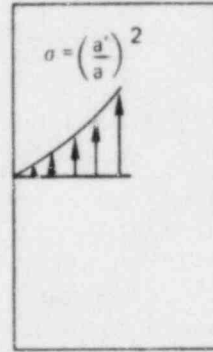
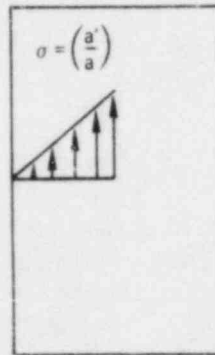
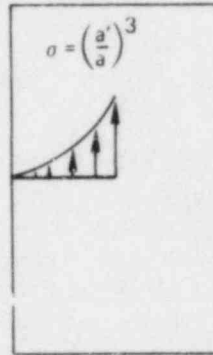
(a) $K_I = K_{I0}$ (c) $K_I = K_{I2}$ (b) $K_I = K_{I1}$ (d) $K_I = K_{I3}$

Fig. 2.4. Crack-surface loading cases for determining 3-D flaw influence coefficients.

where ϕ is the elliptical angle denoting the point on the crack front, and the crack-depth notation (a) has been dropped.

3. CALCULATION AND EVALUATION OF INFLUENCE COEFFICIENTS FOR SPECIFIC 3-D FLAWS

3.1 Computer Codes

For the present study, K_j^* was computed using the three-program system, ORMG¹³ -ADINA¹⁴ -ORVIRT,¹⁵ which addresses linear or nonlinear fracture in 2- or 3-D crack configurations. ORMG¹³ automatically generates a complete 3-D finite element model of the cracked structure and creates data files that have formats compatible with ADINA, which is a structural analysis program. ADINA was modified to allow the application of the crack-face loads shown in Fig. 2.4. Special elements that introduce the appropriate stress singularity are used along the crack front.

ORVIRT acts as a postprocessor of the conventional ADINA analysis. It employs a virtual crack-extension technique for the calculation of energy release rates at specified points along the crack front.

3.2 Mesh Design

Figures 3.1 and 3.2 illustrate a typical ORMG¹³ mesh design for a semielliptical surface flaw and show the mesh in the plane of the flaw and in a plane normal to the fracture surfaces. For this particular design, the number of elements in the azimuthal and axial directions, the number of rings of elements in the ligament from the crack front to the outer wall, the number of elements along the crack front, and the number of elements through the cladding must be included. A geometric progression factor was used with the first three categories of elements.

3.3 Mesh Convergence Studies

In the process of calculating the influence coefficients, careful attention was paid to using adequately converged FE meshes and appropriate cylinder lengths. The number of elements in each category of elements was increased, one category at a time, to the point where the addition of one element in a single category changed the value of K_I by less than 1%. The resultant converged meshes for a 90°, half-length segment of the cylinder had ~8700 degrees of freedom.

Convergence of the K_I values was examined at all points along the crack front, except for the case in which the number of elements along the crack front was varied; for this case, only the K_I value at the deepest point was examined. Also, because convergence was more sensitive to details of the mesh design for the deeper flaws, most of the mesh convergence studies were based on rather deep flaws ($a/w = 0.8$).

DWG. NO. K/G-84-2637
(U)

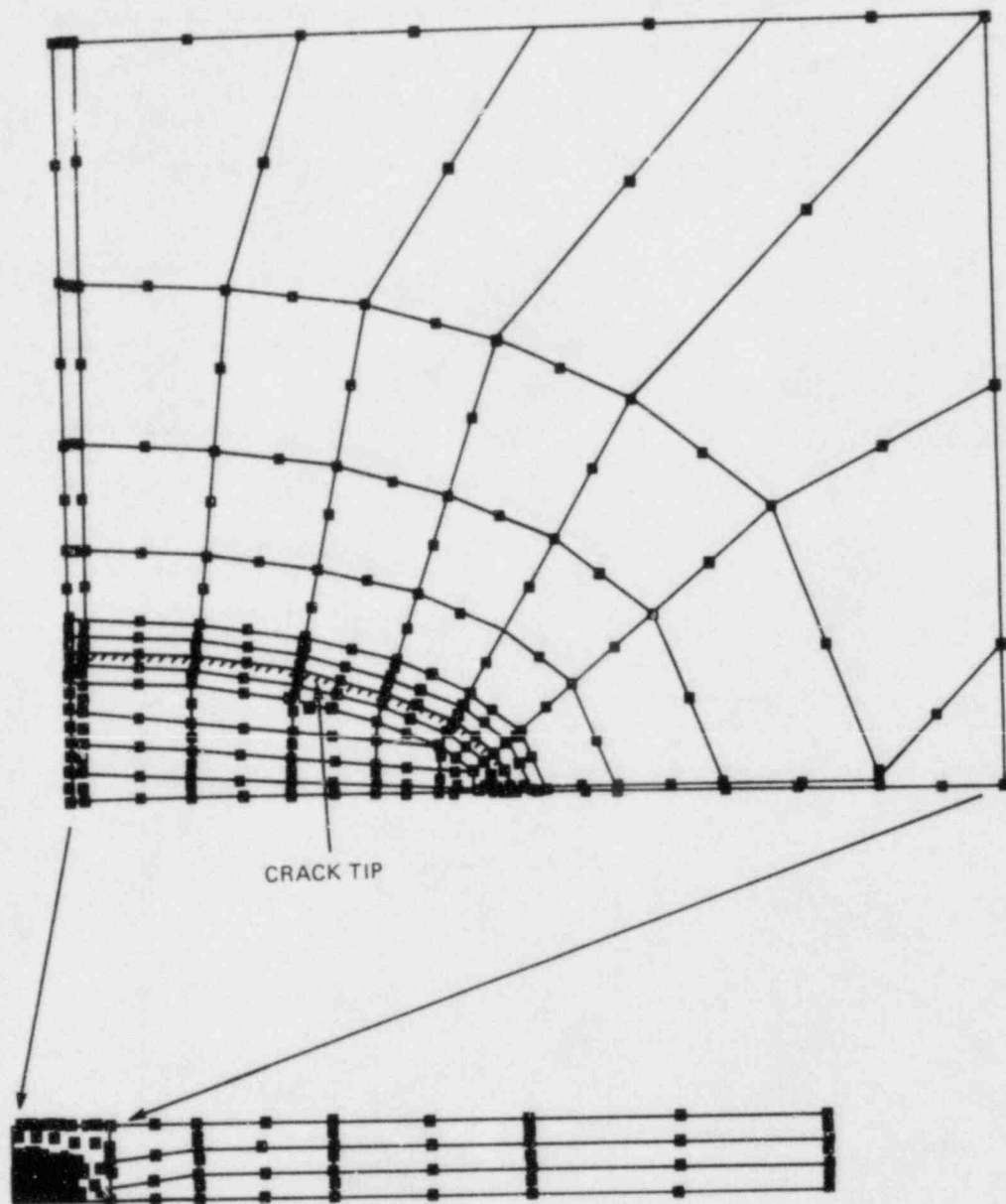


Fig. 3.1. Sample mesh in crack plane for $a/w = 0.2$, $c/a = 2.5$.

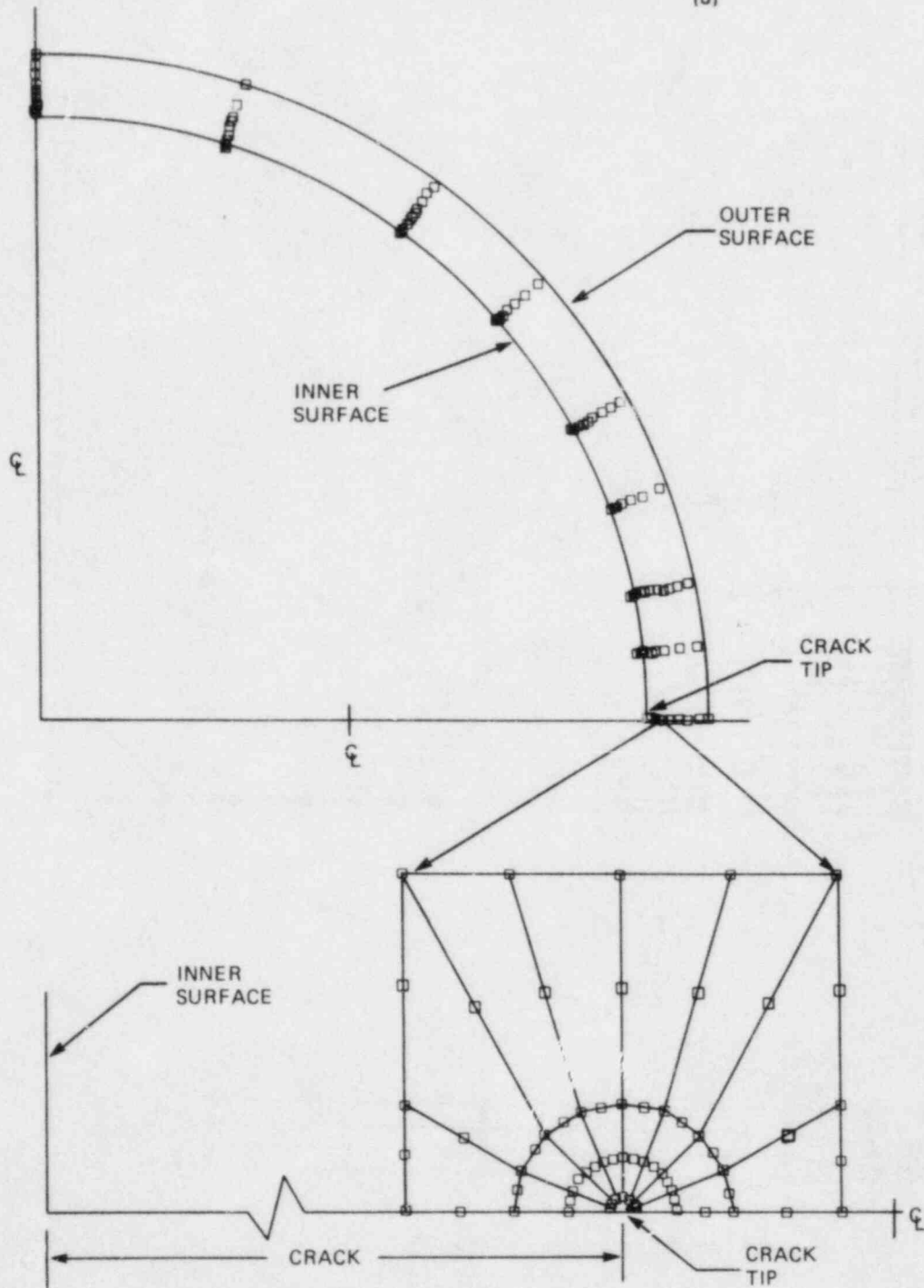


Fig. 3.2. Sample mesh viewed from axial direction.

3.4 90° vs 180° Model

To minimize demands on the computer, only a 90° segment of the cylinder was used in the calculation of the influence coefficients (Fig. 3.3). This corresponds to having flaws at 0° and 180° (two flaws opposite each other); however, as illustrated below, the error in using these same coefficients for a single flaw, which would require a 180° segment to be exact, is reasonably small for the flaws of interest.

The difference in K_I values associated with the 90° and 180° models increases with the length and depth of the flaw. Reference 10 states that the difference for a 2-D flaw with $a/w = 0.8$ is only 2%, but it appeared that this conclusion was based on an analysis that used an inappropriate model. Thus, a separate comparison analysis was performed for a 2-D inner-surface axial flaw in a typical PWR vessel. The 90° and 180° models are shown in Fig. 3.3. The cylinder dimensions were those indicated in this figure, and the thermal loading was that shown in Fig. 3.4. This loading is characteristic of a typical postulated severe thermal transient for a PWR.

Results of the 2-D comparison analysis (Table 3.1) show that for $a/w = 0.8$, the 90° model results in a 30% higher value of K_I . Because this value is rather large, a similar comparison was made for the 2-m flaw with $a/w = 0.8$. For this case, the K_I value for the 90° model was only 4% higher. Because the difference would be even less for shallower flaws of the same length, and because this study was not concerned with 3-D flaw lengths greater than 2 m, it was concluded that for the purposes at hand, the difference between the 90° and 180° models was negligible.

DWG. NO. K/G-84-2534
(U)

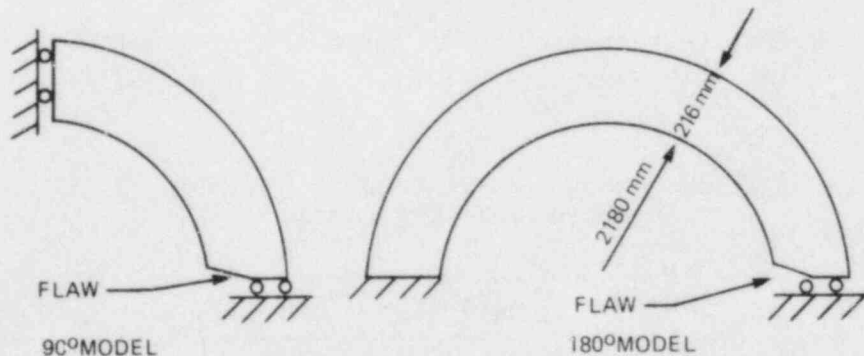


Fig. 3.3. 90° and 180° models used for determining difference in K_I values for single axial flaw and two opposite flaws.

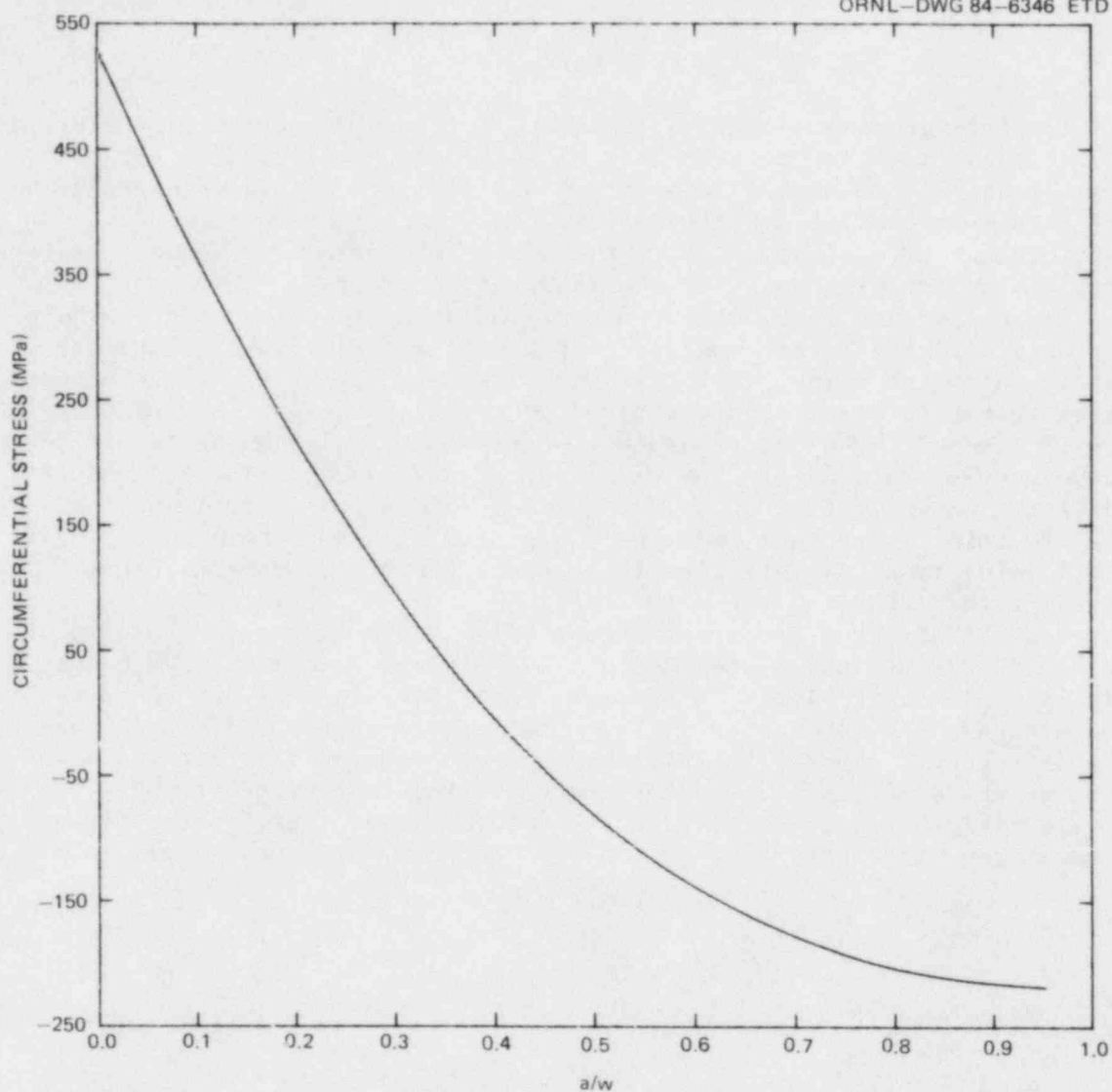


Fig. 3.4. Thermal stress profile in PWR used for comparison calculation of K_I in Table 3.1.

Table 3.1. Comparison of K values for 2-D flaws in 90° and 180° models

a/w	$\frac{K_I(90^\circ) - K_I(180^\circ)}{K_I(180^\circ)} \times 10^2$ (%)
0.1	0.4
0.4	3.5
0.8	30.4

3.5 Length of Cylinder

With regard to cylinder length, a minimum incremental length of cylinder that could be added to the length of the flaw to negate end effects was estimated from Eq. (6) (Ref. 16):

$$\ell = \frac{2\pi}{\beta}, \quad (6)$$

where

$$\beta^4 = \frac{3(1 - \nu^2)}{R_1^2 w^2},$$

R_1 = radius of cylinder,
 w = wall thickness,
 ν = Poisson's ratio.

For the cylinder radial dimensions given in Fig. 3.3, $\ell \approx 3300$ mm. A 3-D analysis, using the 2-m flaw and a typical transient, indicated that this added length was not sufficient to reduce end effects below ~5% at all points on the crack front, and that the required length to reduce end effects below 2% would be greater than the length of a typical PWR vessel between the lower head and the nozzle ring. It was decided that for the 2-m flaw, a cylinder length of 7010 mm would be appropriate. A similar analysis for the 6/1, inner-surface, semielliptical flaw with a maximum fractional depth of 0.2 indicated an appropriate length of 4670 mm. In both cases, the ends of the cylinder were free.

3.6 Adequacy of Third-Order Polynomial to Represent Stress Distribution

The adequacy of a third-order polynomial to represent the stress distribution was investigated by calculating K_I values by both the superposition and direct FE techniques. The first comparison was for the 2-m inner-surface flaw in a PWR with $a/w = 0.6$ and the loading indicated in Fig. 3.5. The results of this comparison analysis indicate a maximum difference of ~1% along the crack front (Fig. 3.6).

The second comparison was for the 1-m, axially oriented, outer-surface flaw in a pressurized-thermal-shock-experiment (PTSE) test vessel ($a/w = 0.1$ and 0.6). The applied load is shown in Fig. 3.7, and the results are given in Fig. 3.8. Again, good agreement was obtained.

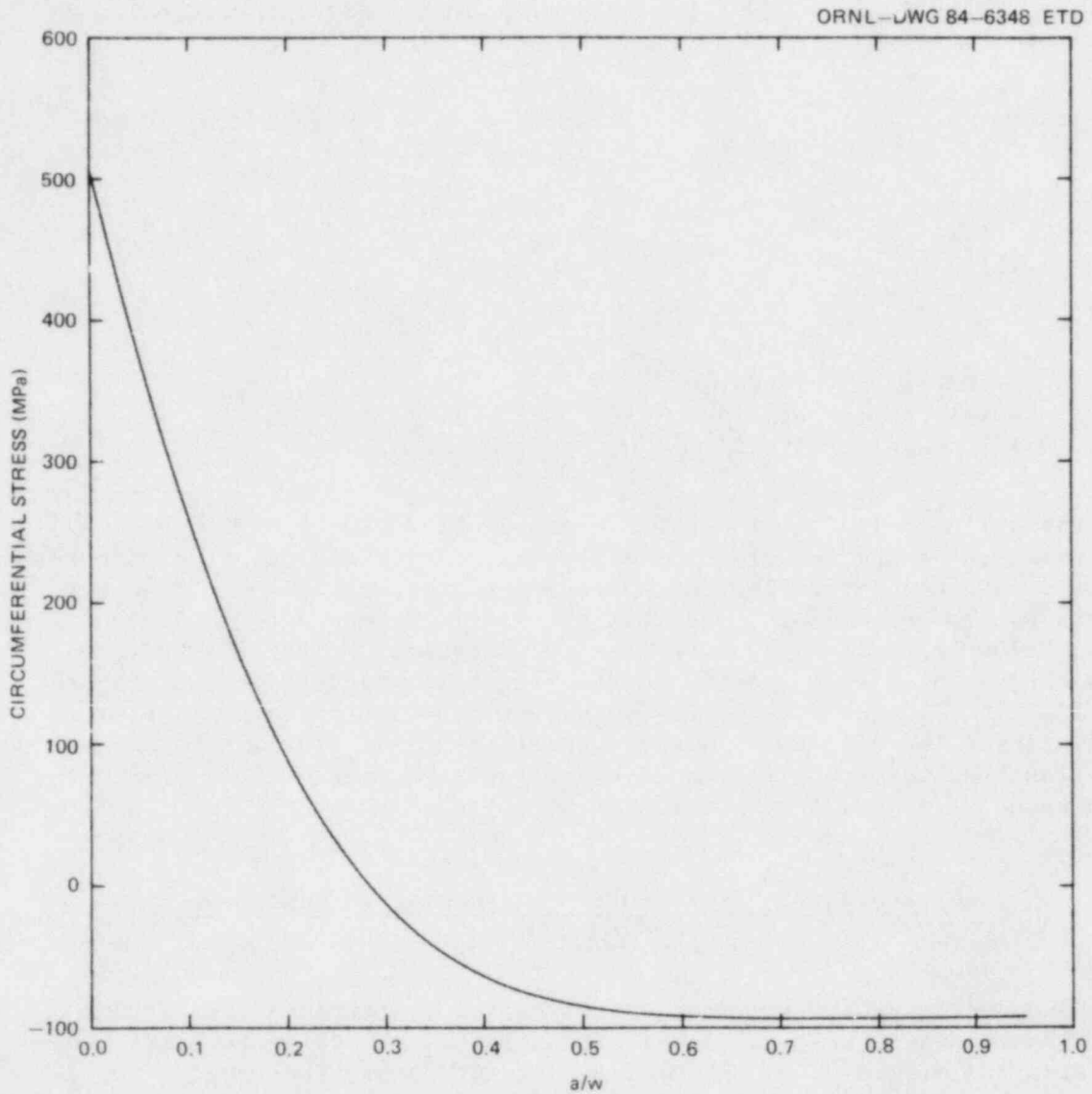


Fig. 3.5. Thermal stress profile in PWR used to calculate K_I given in Fig. 3.6.

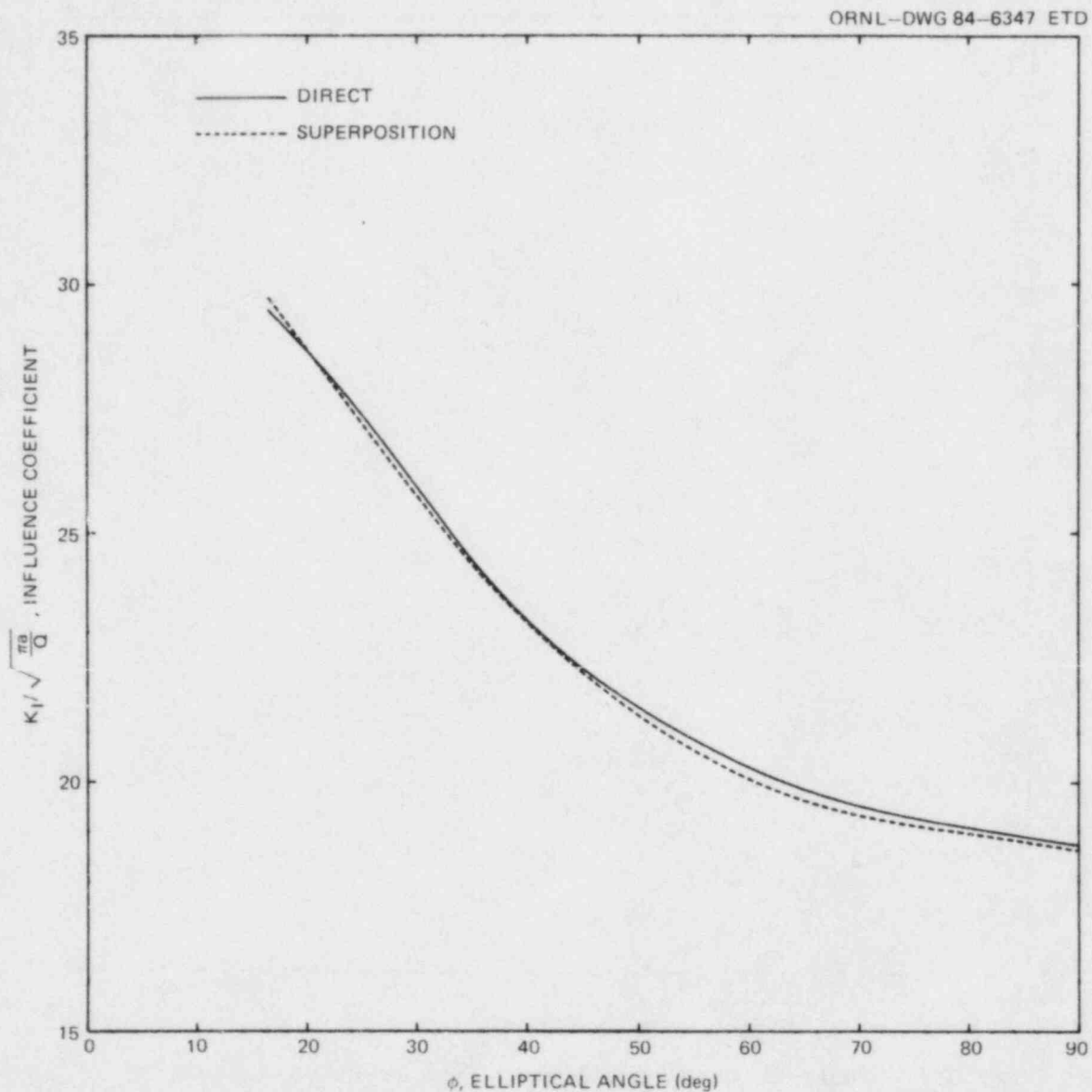


Fig. 3.6. Comparison of K_I values calculated by superposition and direct FE techniques for axially oriented, inner-surface 2-m flaw ($a/w = 0.6$) in PWR vessel during severe thermal transient.

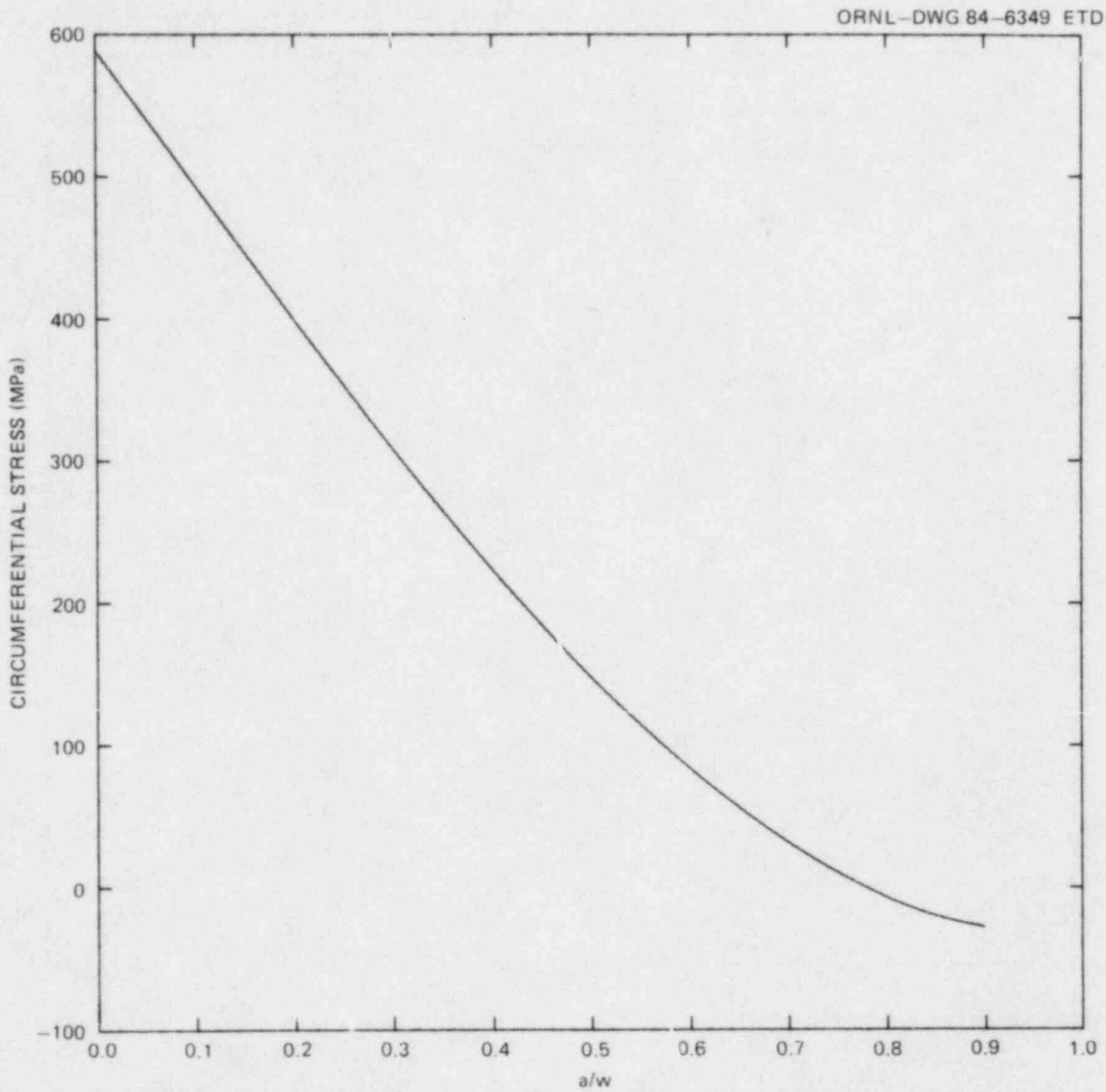


Fig. 3.7. Thermal stress profile in PT3E test vessel used to calculate K_I given in Fig. 3.8.

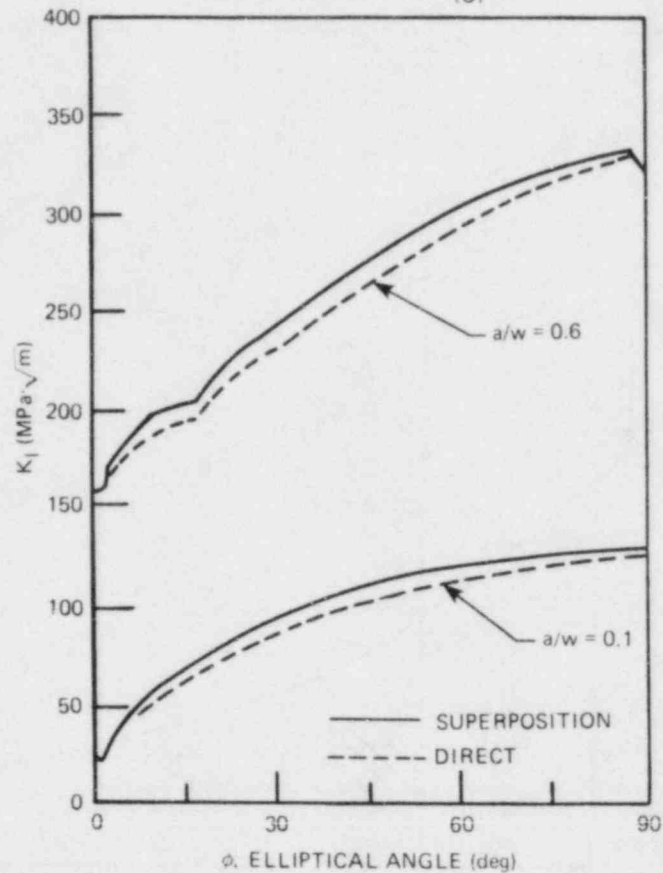


Fig. 3.8. Comparison of 3-D superposition with 3-D direct analysis for axially oriented, outer-surface 1-m flaw in PTSE test vessel.

3.7 Accommodation of Cladding

The presence of a thin layer of stainless steel cladding on the inner surface of PWR pressure vessels has a significant effect on the K_I values for inner-surface flaws because of very high thermal stresses generated in the cladding during a thermal transient. To accommodate the stress discontinuity associated with the cladding, influence coefficients were calculated for the cladding stresses alone; the corresponding K_I value can then be superimposed on the K_I value due to the stresses in the base material. As indicated in Fig. 3.9, this is accomplished by first calculating a K_I value for a continuous-function stress distribution that is obtained by a linear extrapolation into the cladding of the stress distribution in the base material. Then a K_I value is calculated for a stress distribution in the cladding that is obtained by subtracting the extrapolated distribution from the actual distribution in the cladding, which is also assumed to be linear. The total K_I value is simply the sum of the two. Because the stress distribution in the cladding is essentially linear, it is represented by a first-order polynomial.

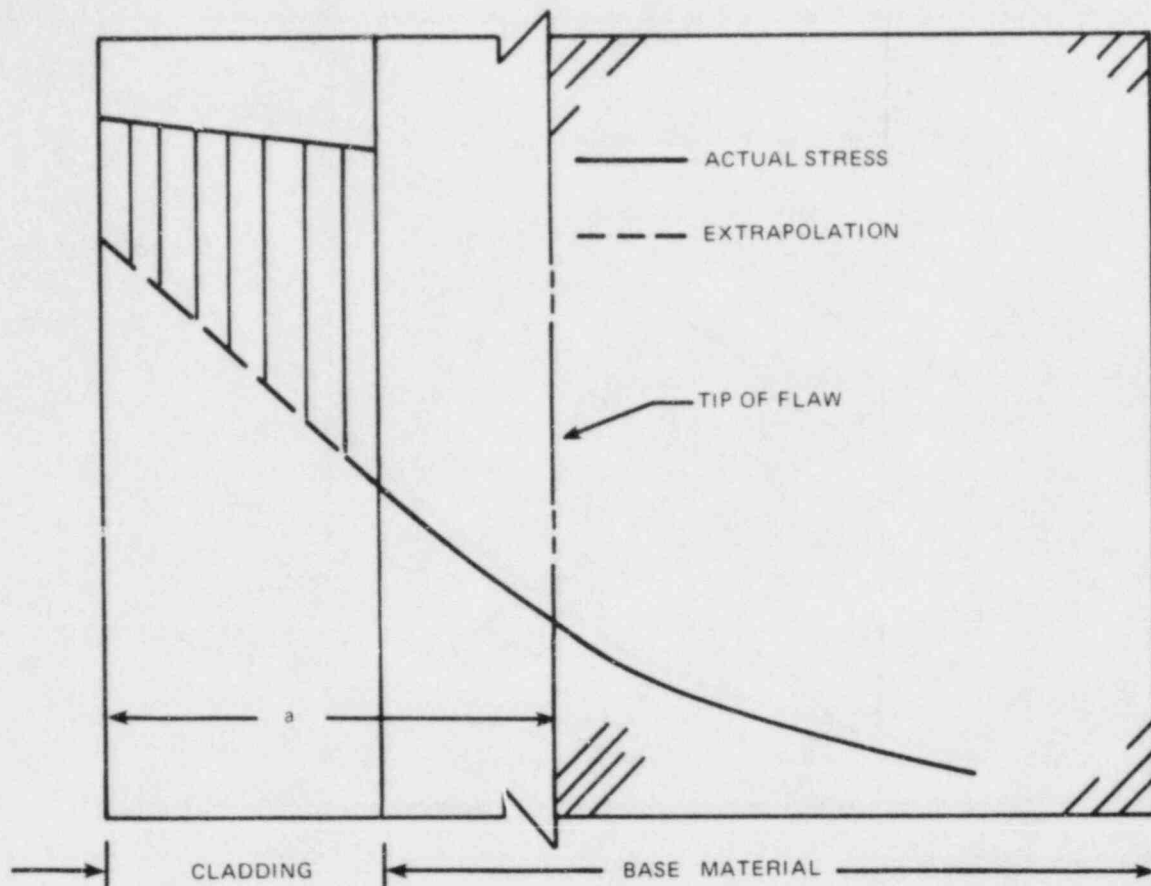


Fig. 3.9. Stress distributions used in superposition techniques for including effect of cladding on K_I .

4. COMPARISON WITH OTHER INVESTIGATORS

A comparison of some of the 3-D influence coefficients derived herein with similar coefficients obtained by other investigators⁸⁻¹⁰ is shown in Figs. 4.1-4.3. (To compare the coefficients with those obtained from the closed-form solution for a buried elliptic flaw in an infinite medium with a uniform stress normal to the crack plane, the influence coefficients in Figs. 4.1-4.3 represent K_I values divided by $\sqrt{\pi a/Q}$, where Q is the square of the complete elliptic integral of the second kind.) As indicated in the figures, the coefficients being compared pertain to axially oriented, inner-surface flaws in a long cylinder with $a/w = 0.2$, 0.5 , and 0.8 ; $c/a = 2.5$ and 3.0 ; and $R_0/R_1 = 1.10$ (refer to Fig. 2.3).

The results of the comparison indicate good agreement, with our values being slightly higher and the biggest difference (7%) at the deepest point occurring for the cubic stress distribution. Furthermore, for a shallow flaw ($a/w = 0.2$, see Appendix B) the influence coefficients for a uniform stress and $\phi = \pi/2$ are ~ 1.10 . This is consistent with estimates of the front-face correction factor that is applied to the buried-

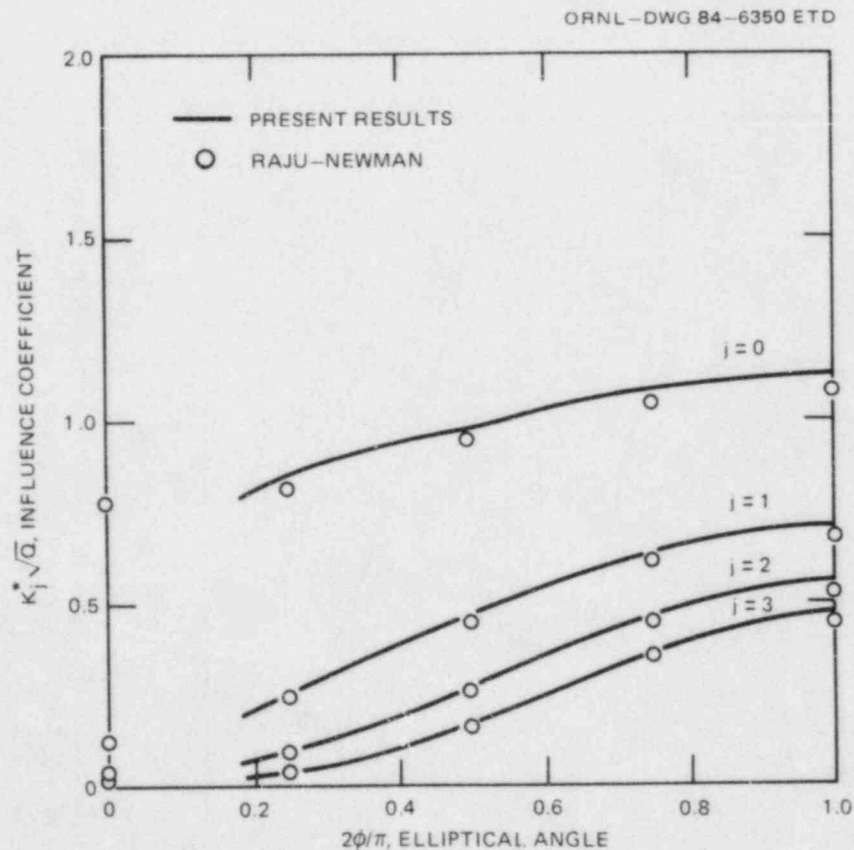


Fig. 4.1. Influence coefficients for longitudinal semielliptical crack on inner surface of cylinder: $a/w = 0.2$, $c/a = 2.5$, $R_0/R_1 = 1.1$.

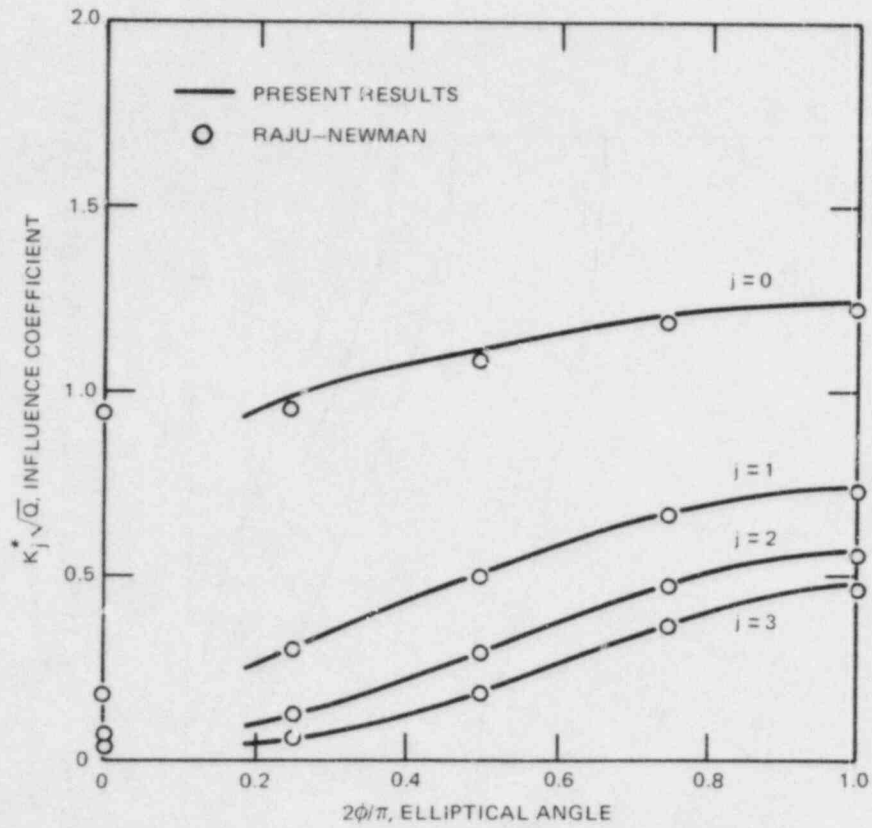


Fig. 4.2. Influence coefficients for longitudinal semielliptical crack on inner surface of cylinder: $a/w = 0.5$, $c/a = 2.5$, $R_o/R_i = 1.1$.

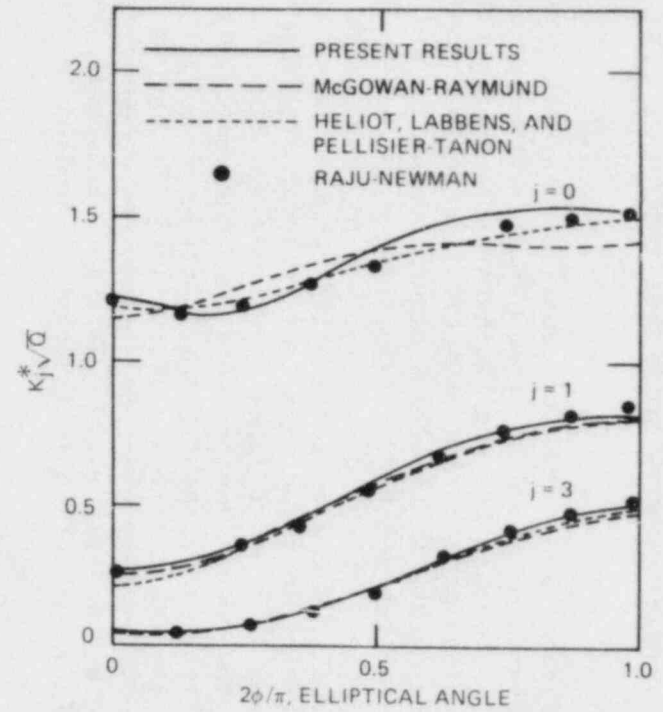


Fig. 4.3. Influence coefficients for longitudinal semielliptical crack on inner surface of cylinder: $a/w = 0.8$, $c/a = 3$, $R_o/R_i = 1.1$.

ellipse K_I value to obtain the K_I value for a semielliptical surface flaw in a semi-infinite medium.¹⁷ For deeper flaws, the finiteness of the wall becomes apparent; that is, the coefficients become larger than those for the semi-infinite medium.

5. INFLUENCE COEFFICIENTS FOR SPECIFIC APPLICATIONS

5.1 Pressurized-Water Reactor

Flaws in a PWR pressure vessel are most likely to be located in the welds that join the segments of the vessel. For most of the vessels in operation today, radiation embrittlement is greater in the welds than in the base material because of higher concentrations of copper in the welds. Thus, although a flaw may extend in length as the result of an overcooling accident (OCA), the length of the flaw tends to be limited to the length of the weld. For many of the plate-type vessels, which have both axial and circumferential welds in the belt-line region, the length of the axial welds is ~2 m, which is equal to the height of a shell course. Recent calculations¹⁸ indicate that the stress-intensity factor for a deep axial flaw of this length is substantially less than for an infinitely long (2-D) flaw, which has been used extensively in the evaluation of vessel integrity during OCAs. Thus, replacement of the 2-D axial flaw with the 2-m axial flaw in crack-growth models could represent a benefit in terms of projected vessel lifetime. For this reason, influence coefficients for 2-m semielliptical, axial flaws were calculated and are included in Appendix A.

Another finite-length flaw of interest, particularly for initial flaws, is a semielliptical flaw with a surface-length-to-depth ratio of 6/1. There is no particular technical justification for using this specific initial flaw in the analysis of OCAs except that, presumably, initial flaws are much more likely to be short than long. With this in mind, and also because other investigators have included the 6/1 flaw in their studies, coefficients for a 6/1 flaw were calculated and are given in Appendix B.

5.2 Pressurized-Thermal-Shock-Experiment Test Vessel

An experimental program¹⁹ is under way at Oak Ridge National Laboratory (ORNL) to examine the response of surface-cracked test vessels to time-dependent combined pressure and thermal loadings similar to those calculated for PWR postulated OCAs. The PTSE facility (Fig. 5.1) at ORNL subjects a heated thick-walled cylindrical test vessel with a long axial flaw on the outer surface to a sudden flow of chilled liquid on the outside surface and to a prescribed pressure transient on the inner surface. Data from these experiments will be used to help validate methods of fracture analysis that are useful in predicting crack behavior for certain accident scenarios.

Influence coefficients were calculated for the flaw in Fig. 5.1, assuming that the flaw was semielliptical in shape and that it would grow in depth but not length. Coefficients were obtained for several crack depths and several positions on the crack front. These values are presented in Appendix C.

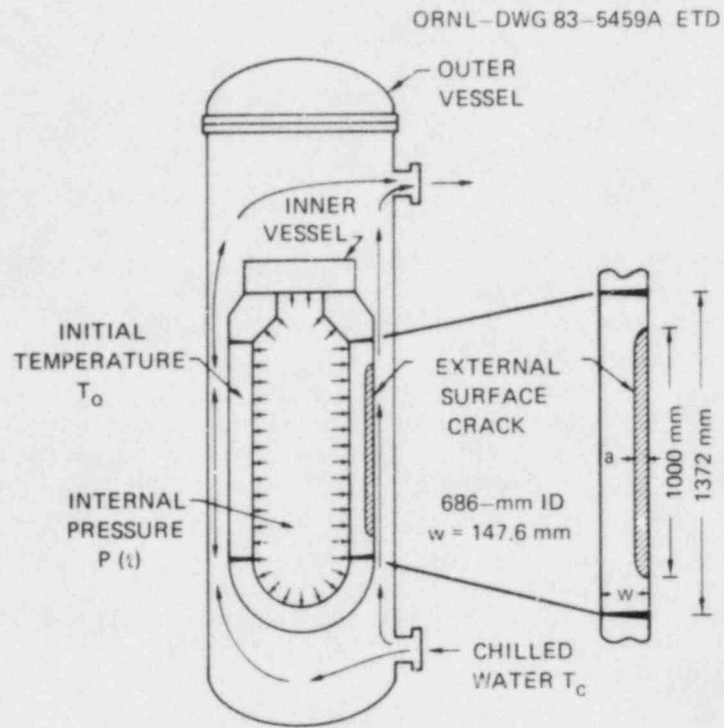


Fig. 5.1. PTSE test vessel with longitudinal outer-surface crack.

REFERENCES

1. R. D. Cheverton, "Thermal Shock Studies Associated with Injection of Emergency Core Coolant Following a Loss of Coolant Accident in PWR's," *Nuclear Safety* 19(1), 10-20 (January-February 1978).
2. D. J. Ayers and W. F. Siddall, *Finite Element Analysis of Structural Integrity of a Reactor Pressure Vessel During Emergency Core Cooling*, Report A-70-19-2, Combustion Engineering, Inc., January 1970.
3. S. K. Iskander, *Two Finite Element Techniques for Computing Mode I Stress Intensity Factors in Two- or Three-Dimensional Problems*, NUREG/CR-1499 (ORNL/NUREG/CSD/TM-14), Computer Sciences Division, Union Carbide Corp. Nuclear Div., Oak Ridge Natl. Lab., February 1981.
4. H. G. DeLorenzi, "3-D Elastic-Plastic Fracture Analysis with ADINA," *Computers and Structures* 13, 613-21 (1981).
5. S. N. Atluri et al., *ORFLAW: A Finite Element Program for Direct Evaluation of K-Factors for User-Defined Flaws in Plate, Cylinders and Pressure-Vessel Nozzle Corners*, NUREG/CR-2492 (ORNL/CSD/TM-165), Union Carbide Corp. Nuclear Div., Oak Ridge Natl. Lab., April 1982.
6. B. R. Bass et al., "Applications of Energy Release Rate Techniques to Part-Through Cracks in Experimental Pressure Vessels," *J. Pressure Vessel Tech.* 104, 308-16 (November 1983).
7. C. B. Buchalet and W. H. Bamford, "Stress Intensity Factor Solutions for Continuous Surface Flaws in Reactor Pressure Vessels," pp. 385-402 in *Mechanics of Crack Growth*, ASTM STP 590, American Society for Testing and Materials, 1976.
8. J. Heliot, R. C. Labbens, and A. Pellissier-Tanon, "Semi-Elliptical Cracks in a Cylinder Subjected to Stress Gradients," pp. 341-64 in *Fracture Mechanics*, ASTM STP 677, ed. C. W. Smith, American Society for Testing and Materials, 1979.
9. J. J. McGowan and M. Raymund, "Stress Intensity Factor Solutions for Internal Longitudinal Semi-Elliptical Surface Flaws in a Cylinder Under Arbitrary Loadings," pp. 365-80 in *Fracture Mechanics*, ASTM STP 677, ed. C. W. Smith, American Society for Testing and Materials, 1979.
10. I. S. Raju and J. C. Newman, Jr., "Stress Intensity Factor Influence Coefficients for Internal and External Surface Cracks in Cylindrical Vessels," pp. 37-48 in *Aspects of Fracture Mechanics in Pressure Vessels and Piping*, ASME Pub. PVP 58, American Society of Mechanical Engineers, 1982.

11. S. K. Iskander, R. D. Cheverton, and D. G. Ball, *OCA-1, A Code for Calculating the Behavior of Flaws on the Inner Surface of a Pressure Vessel Subjected to Temperature and Pressure Transients*, NUREG/CR-2113 (ORNL/NUREG-84), Union Carbide Corp. Nuclear Div., Oak Ridge Natl. Lab., August 1981.
12. D. G. Ball et al., *OCA-II, A Code for Calculating the Behavior of 2-D and 3-D Surface Flaws in a Pressure Vessel Subjected to Temperature and Pressure Transients*, NUREG/CR-3491 (ORNL-5934), Union Carbide Corp. Nuclear Div., Oak Ridge Natl. Lab., February 1984.
13. B. R. Bass and J. W. Bryson, *Applications of Energy Release Rate Techniques to Part-Through Cracks in Plates and Cylinders, Vol. 1. ORMGEN-3D: A Finite Element Mesh Generator for 3-Dimensional Crack Geometries*, NUREG/CR-2997, Vol. 1 (ORNL/TM-8527/V1), Union Carbide Corp. Nuclear Div., Oak Ridge Natl. Lab., December 1982.
14. K. J. Bathe, *ADINA - A Finite Element Program for Automatic Dynamic Incremental Nonlinear Analysis*, Report 82448-1, Mechanical Engineering Department, Massachusetts Institute of Technology, December 1978.
15. B. R. Bass and J. W. Bryson, *Applications of Energy Release Rate Techniques to Part-Through Cracks in Plates and Cylinders, Vol. 2. ORVIRT: A Finite Element Program for Energy Release Rate Calculations for 2-Dimensional and 3-Dimensional Crack Models*, NUREG/CR-2997, Vol. 2 (ORNL/TM-8527/V2), Union Carbide Corp. Nuclear Div., Oak Ridge Natl. Lab., February 1983.
16. S. Timoshenko, *Theory of Plates and Shells*, McGraw-Hill, New York, 1940.
17. Hiroshi Tada, P. C. Paris, and G. R. Irwin, *The Stress Analysis of Cracks Handbook*, Del Research Corporation, Hellertown, Pa, 1973.
18. J. G. Merkle et al., "Fracture Mechanics Analysis and Investigations," in *Heavy-Section Steel Technology Program Quart. Prog. Rep. July-September 1982*, NUREG/CR-2751, Vol. 3 (ORNL/TM-8369/V3), Union Carbide Corp. Nuclear Div., Oak Ridge Natl. Lab., January 1983.
19. R. H. Bryan and R. W. McCulloch, "Pressurized-Thermal-Shock Studies," in *Heavy-Section Steel Technology Program Quart. Prog. Rep. October-December 1982*, NUREG/CR-2751, Vol. 3 (ORNL/TM-8369/V4), Union Carbide Corp. Nuclear Div., Oak Ridge Natl. Lab., May 1983.

Appendix A

INFLUENCE COEFFICIENTS FOR THE 2-m FLAW IN A PWR

Influence coefficients are included for the 2-m flaw [an axially oriented, 1.83-m-long semielliptical inner-surface flaw in a cylinder with $R_1 = 2184.4$ mm, $w = 215.9$ mm, and $l = 7010$ mm; the cladding thickness is 5.4 mm (Table A.1)]. The coefficients are presented in terms of G_j , where $G_j = K_j^* \sqrt{Q}$, and Q is the square of the complete elliptic integral of the second kind. Figures A.1 and A.2 are graphs of the influence coefficients at the deepest point on the crack front vs a/w for the unclad cylinder and for the cladding area.

Table A.1. Influence coefficients for the
2-m flaw in a PWR

a/w	$2\phi/\pi$	Unclad cylinder				Cladding	
		G_0	G_1	G_2	G_3	G_0	G_1
0.200	0.184	0.641	0.112	0.031	0.010	0.172	0.087
	0.263	0.753	0.197	0.062	0.014	0.161	0.082
	0.421	0.935	0.356	0.167	0.080	0.131	0.066
	0.579	1.082	0.516	0.306	0.195	0.120	0.061
	0.737	1.188	0.646	0.441	0.327	0.119	0.060
	0.895	1.249	0.723	0.530	0.423	0.123	0.062
	1.000	1.283	0.752	0.573	0.485	0.129	0.065
0.250	0.184	0.656	0.119	0.032	0.009	0.144	0.073
	0.263	0.778	0.208	0.069	0.022	0.134	0.067
	0.421	0.974	0.369	0.175	0.088	0.112	0.057
	0.579	1.131	0.531	0.315	0.203	0.107	0.054
	0.737	1.245	0.663	0.451	0.335	0.108	0.054
	0.895	1.313	0.742	0.540	0.431	0.112	0.056
	1.000	1.345	0.770	0.580	0.485	0.117	0.058
0.300	0.184	0.681	0.129	0.035	0.011	0.126	0.063
	0.263	0.813	0.221	0.077	0.029	0.116	0.059
	0.421	1.020	0.385	0.184	0.095	0.101	0.051
	0.579	1.186	0.548	0.325	0.210	0.099	0.049
	0.737	1.309	0.683	0.462	0.343	0.101	0.050
	0.895	1.384	0.765	0.552	0.440	0.105	0.052
	1.000	1.414	0.793	0.590	0.489	0.109	0.054
0.400	0.184	0.752	0.157	0.047	0.018	0.104	0.052
	0.263	0.899	0.251	0.093	0.040	0.097	0.049
	0.421	1.124	0.420	0.204	0.109	0.088	0.044
	0.579	1.309	0.589	0.347	0.226	0.089	0.044
	0.737	1.449	0.729	0.486	0.359	0.093	0.046
	0.895	1.535	0.815	0.578	0.457	0.096	0.048
	1.000	1.560	0.842	0.613	0.501	0.099	0.049
0.500	0.184	0.855	0.194	0.064	0.028	0.093	0.047
	0.263	1.016	0.291	0.113	0.052	0.088	0.044
	0.421	1.255	0.464	0.227	0.123	0.083	0.041
	0.597	1.454	0.638	0.372	0.242	0.085	0.042
	0.737	1.605	0.781	0.513	0.377	0.089	0.044
	0.895	1.698	0.870	0.607	0.475	0.092	0.046
	1.000	1.717	0.896	0.640	0.516	0.094	0.047
0.600	0.184	0.983	0.238	0.085	0.040	0.089	0.044
	0.263	1.155	0.337	0.136	0.065	0.085	0.042
	0.421	1.400	0.513	0.251	0.139	0.080	0.040
	0.579	1.603	0.687	0.398	0.258	0.083	0.041
	0.737	1.753	0.831	0.538	0.393	0.086	0.043
	0.895	1.842	0.919	0.632	0.491	0.088	0.044
	1.000	1.857	0.944	0.664	0.530	0.089	0.044

Table A.1 (continued)

a/w	$2\phi/\pi$	Unclad cylinder				Cladding	
		G_0	G_1	G_2	G_3	G_0	G_1
0.700	0.184	1.135	0.288	0.109	0.053	0.087	0.044
	0.263	1.311	0.387	0.160	0.079	0.084	0.042
	0.421	1.552	0.562	0.276	0.153	0.080	0.040
	0.579	1.746	0.734	0.422	0.273	0.081	0.041
	0.737	1.880	0.875	0.562	0.408	0.083	0.041
	0.895	1.955	0.961	0.655	0.507	0.083	0.041
	1.000	1.968	0.986	0.688	0.546	0.083	0.041
0.800	0.184	1.290	0.336	0.131	0.066	0.086	0.043
	0.263	1.463	0.435	0.182	0.092	0.082	0.041
	0.421	1.675		0.295	0.164	0.078	0.039
	0.579	1.837	0.706	0.438	0.283	0.078	0.039
	0.737	1.954	0.908	0.582	0.422	0.076	0.038
	0.895	2.014	0.998	0.682	0.527	0.074	0.037
	1.000	2.049	1.034	0.722	0.573	0.075	0.038
0.900	0.184	1.449	0.383	0.152	0.077	0.086	0.043
	0.263	1.612	0.480	0.203	0.102	0.082	0.041
	0.421	1.789	0.639	0.312	0.174	0.077	0.038
	0.579	1.920	0.802	0.459	0.296	0.073	0.036
	0.737	2.021	0.959	0.619	0.449	0.066	0.033
	0.895	2.091	1.084	0.751	0.582	0.061	0.031
	1.000	2.169	1.149	0.814	0.648	0.061	0.031

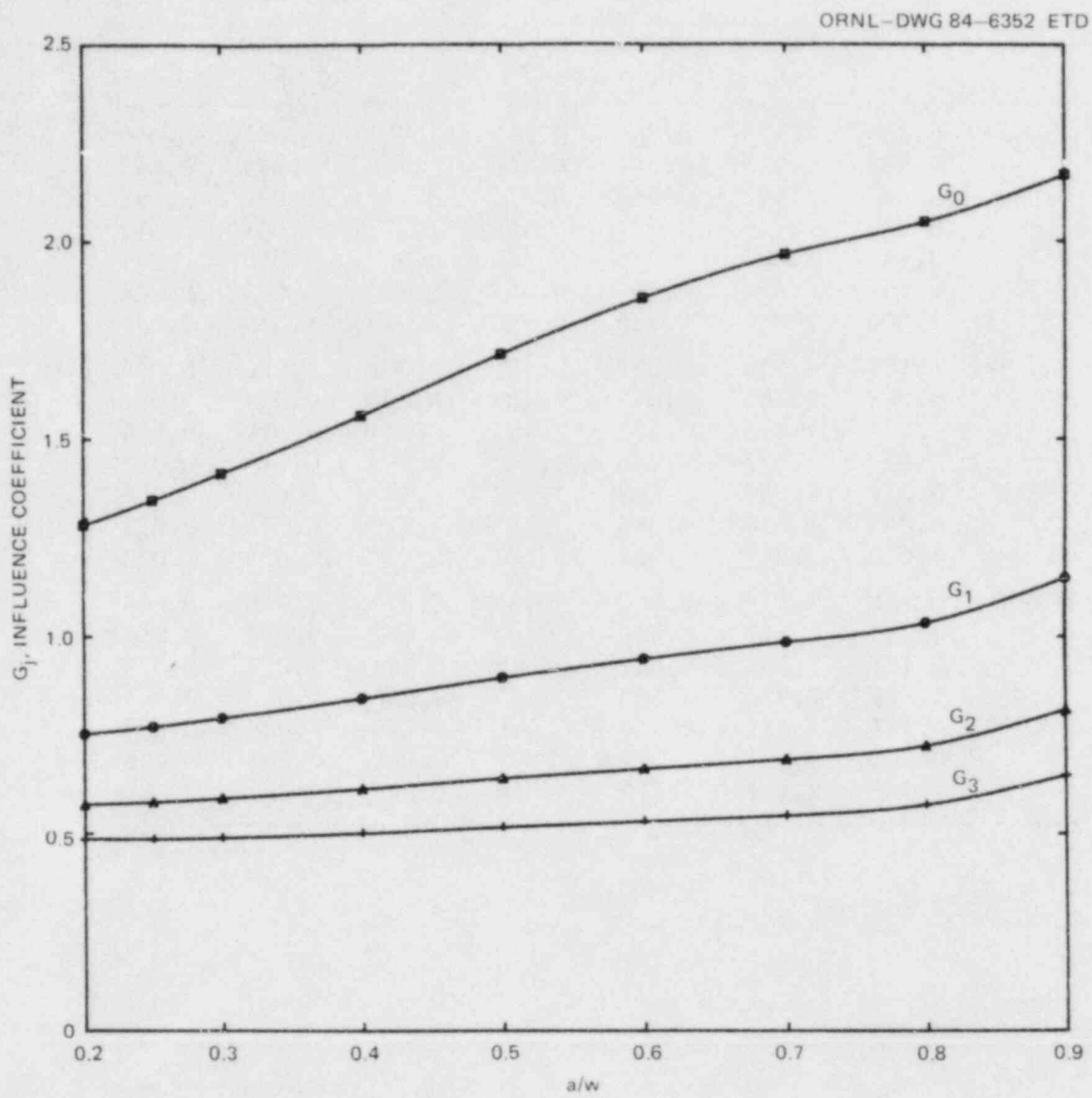


Fig. A.1. Influence coefficients for 2-m flaw at $\phi = 90^\circ$.

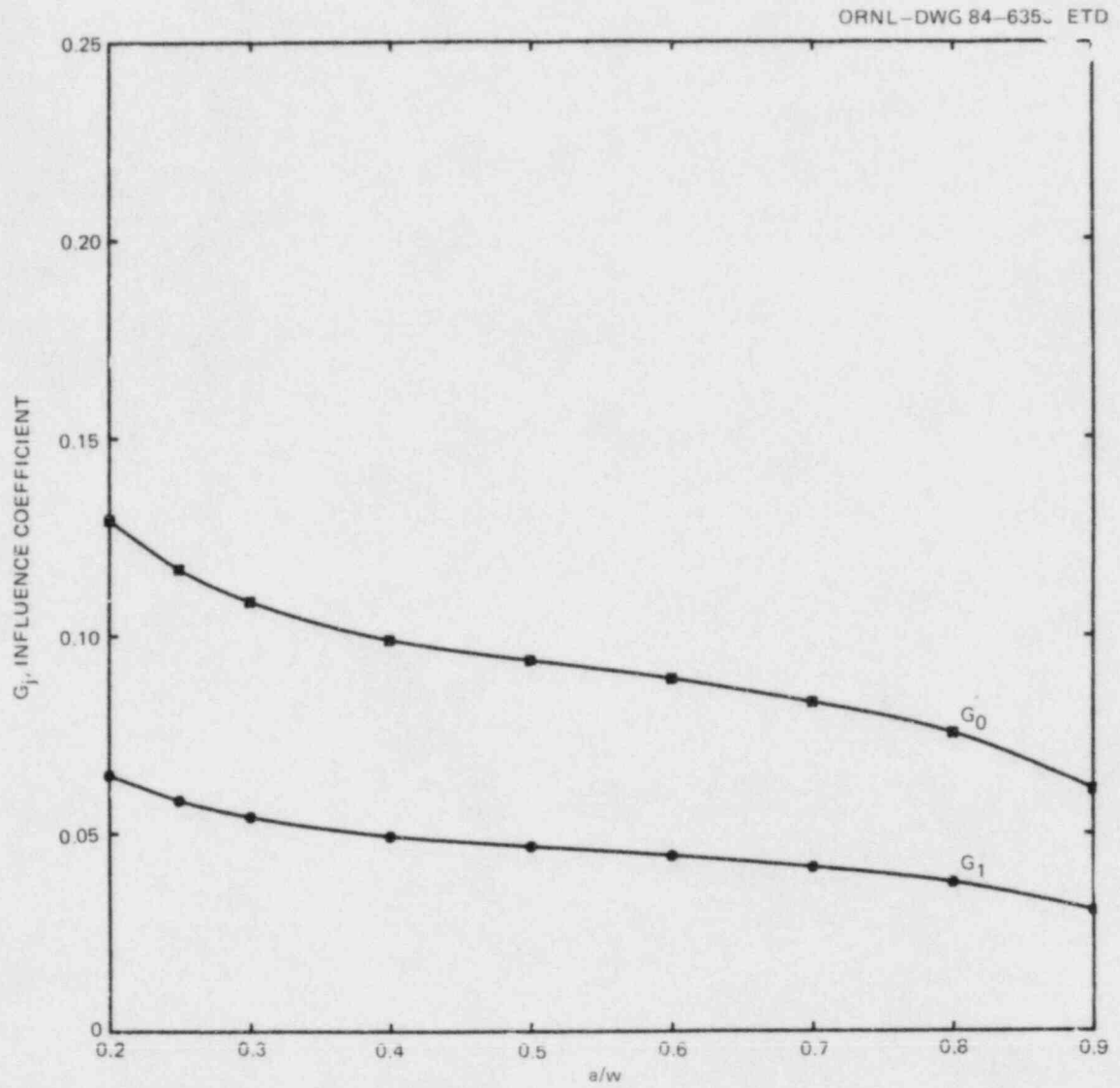


Fig. A.2. Cladding influence coefficients for 2-m flaw at $\phi = 90^\circ$.

Appendix B

INFLUENCE COEFFICIENTS FOR THE 6/1 FLAW IN A PWR

Influence coefficients are included for the 6/1 flaw [an axially oriented, inner-surface flaw in a cylinder with a surface length-to-depth ratio of 6 and with $R_1 = 2184.4$ mm, $w = 215.9$ mm, and $l = 4670$ mm; the cladding thickness is 5.4 mm (Table B.1)]. The coefficients are presented in terms of G_j where $G_j = K_j^* \sqrt{Q}$, and Q is the square of the complete elliptic integral of the second kind. Figure B.1 is a graph of the influence coefficients at the deepest point on the crack front vs a/w for the unclad cylinder.

Table B.1. Influence coefficients for the 6/1 flaw in a PWR

a/w	$2\phi/\pi$	Unclad cylinder				Cladding	
		G_0	G_1	G_2	G_3	G_0	G_1
0.050	1.000	1.180	0.779	0.611	0.515	a	a
0.075	0.184	0.776	0.173	0.051	0.019	a	a
	0.263	0.874	0.253	0.096	0.042	a	a
	0.421	0.977	0.398	0.201	0.111	a	a
	0.579	1.040	0.538	0.336	0.227	a	a
	0.737	1.087	0.651	0.466	0.359	a	a
	0.895	1.116	0.717	0.551	0.455	a	a
	1.000	1.126	0.737	0.579	0.489	a	a
0.100	0.184	0.752	0.173	0.053	0.020	a	a
	0.263	0.843	0.250	0.097	0.043	0.242	0.131
	0.421	0.938	0.390	0.199	0.111	0.192	0.105
	0.579	1.008	0.525	0.330	0.224	0.159	0.086
	0.737	1.066	0.635	0.456	0.352	0.153	0.081
	0.895	1.102	0.701	0.538	0.445	0.159	0.083
	1.000	1.114	0.721	0.565	0.478	0.163	0.085
0.150	0.184	0.746	0.177	0.056	0.022	0.180	0.093
	0.263	0.830	0.252	0.099	0.045	0.171	0.089
	0.421	0.923	0.387	0.199	0.111	0.127	0.066
	0.579	1.003	0.519	0.326	0.222	0.112	0.058
	0.737	1.070	0.627	0.448	0.347	0.113	0.058
	0.895	1.110	0.691	0.528	0.437	0.117	0.060
	1.000	1.122	0.710	0.555	0.469	0.120	0.061
0.200	0.184	0.751	0.182	0.059	0.024	0.147	0.075
	0.263	0.834	0.256	0.101	0.046	0.134	0.069
	0.421	0.928	0.388	0.199	0.112	0.100	0.051
	0.579	1.013	0.518	0.325	0.221	0.092	0.047
	0.737	1.081	0.624	0.445	0.344	0.094	0.047
	0.895	1.120	0.687	0.524	0.433	0.095	0.048
	1.000	1.132	0.706	0.550	0.465	0.097	0.049

^aNot available at the time of this writing.

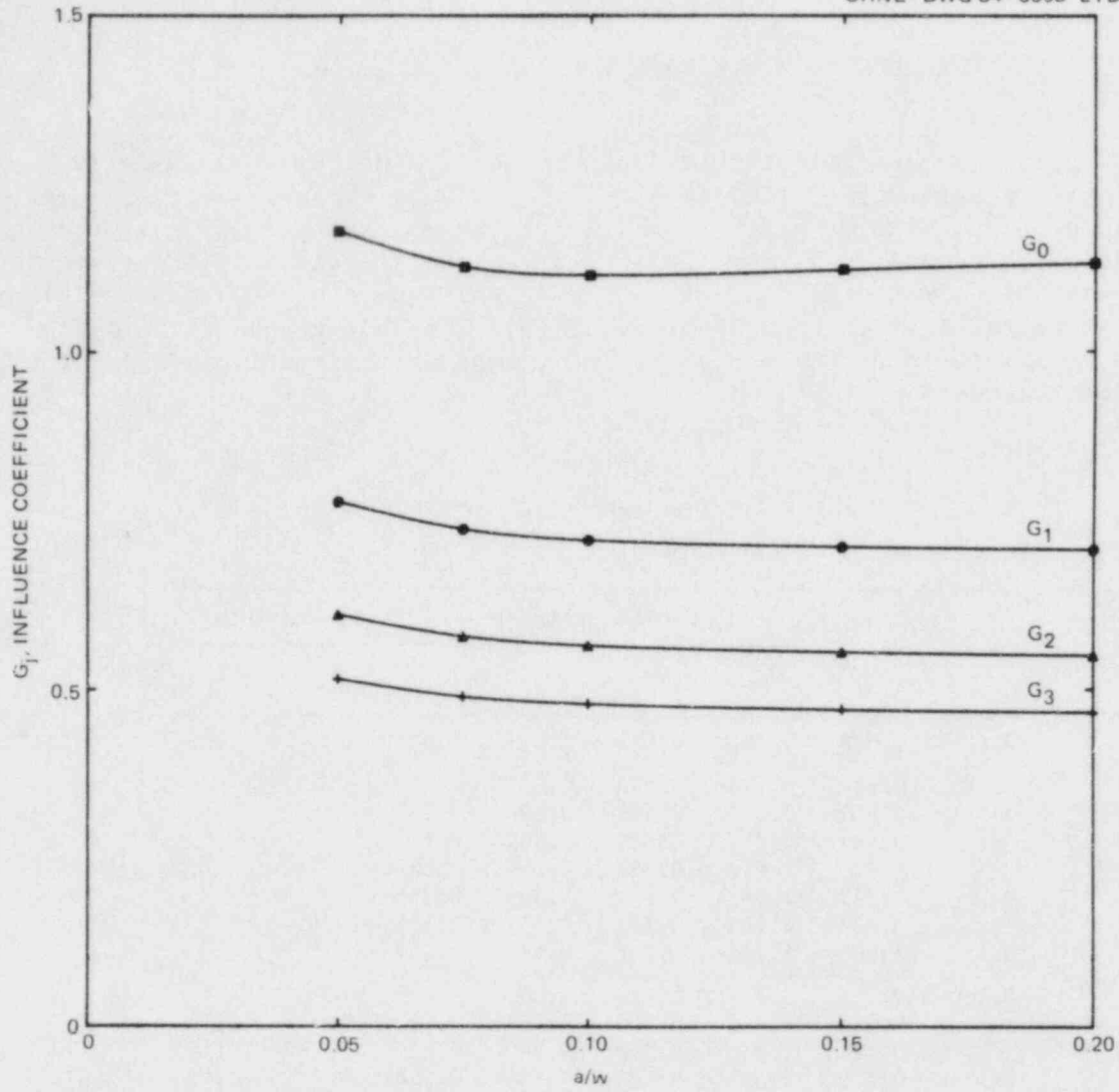


Fig. B.1. Influence coefficients for 6/1 flaw at $\phi = 90^\circ$.

Appendix C

INFLUENCE COEFFICIENTS FOR THE 1-m FLAW
IN A PTSE VESSEL

Influence coefficients are included for the 1-m flaw [an axially oriented, 1.0-m-long, semielliptical, outer-surface flaw in a cylinder with $R_1 = 342.9$ mm and $w = 152.4$ mm (Table C.1)]. The coefficients are presented in terms of G_j where $G_j = K_j^* \sqrt{Q}$, and Q is the square of the complete elliptic integral of the second kind. Figure C.1 is a graph of the influence coefficients at the deepest point on the crack front vs a/w .

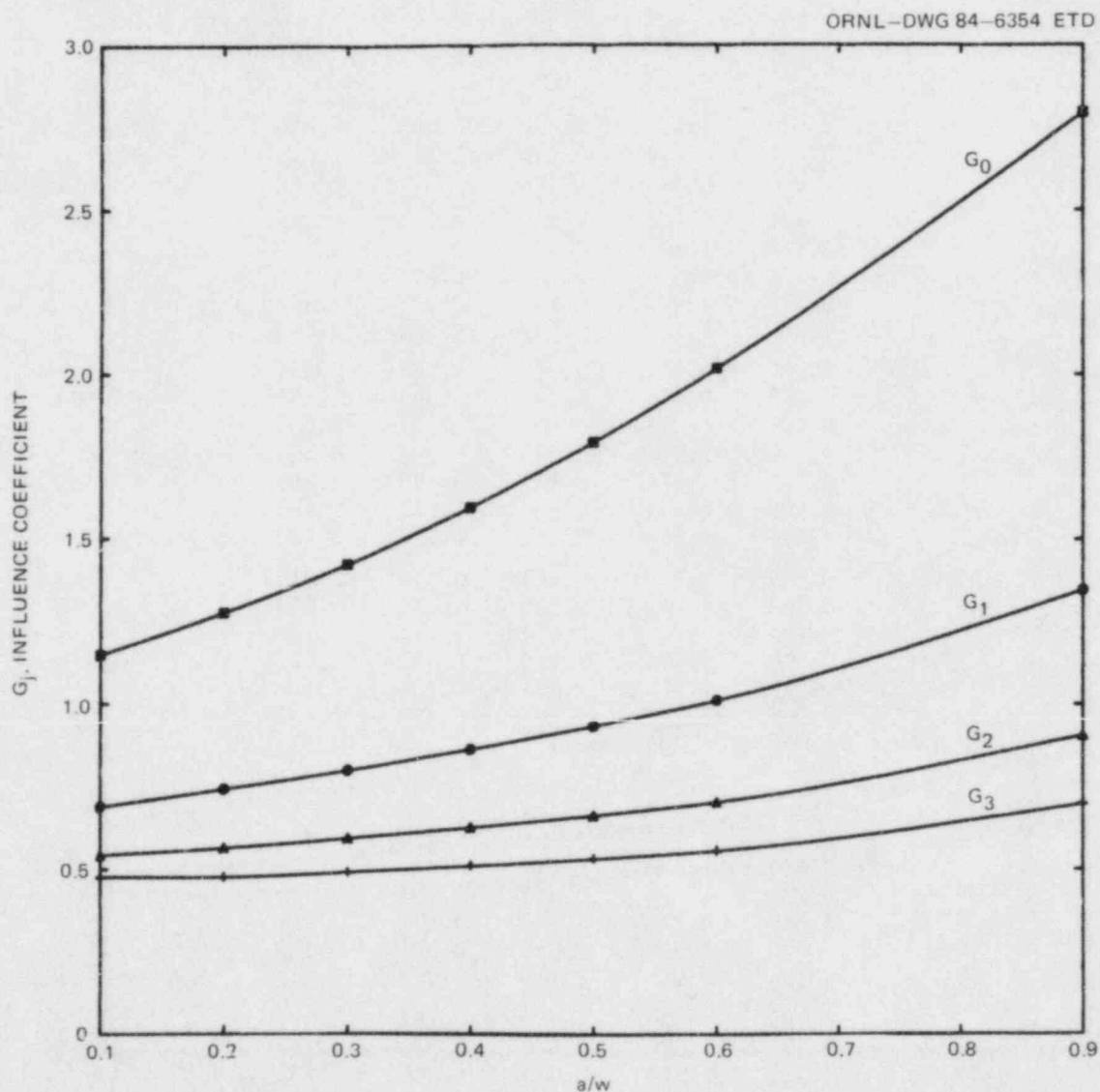


Fig. C.1. Influence coefficients for 1-m outer-surface flaw at deepest point ($\phi = 90^\circ$).

Table C.1. Influence coefficients for the
1-m flaw in a PTSE test vessel

a/w	$2\phi/\pi$	G_0	G_1	G_2	G_3
0.100	0.105	0.457	0.052	0.000	0.000
	0.263	0.695	0.175	0.042	0.000
	0.421	0.873	0.325	0.144	0.054
	0.579	0.994	0.471	0.275	0.167
	0.737	1.077	0.589	0.402	0.293
	0.895	1.124	0.660	0.485	0.385
	1.000	1.148	0.688	0.543	0.476
0.200	0.105	0.505	0.065	0.009	0.000
	0.263	0.744	0.192	0.060	0.015
	0.421	0.935	0.349	0.163	0.080
	0.579	1.082	0.506	0.301	0.193
	0.737	1.189	0.636	0.435	0.324
	0.895	1.253	0.716	0.524	0.421
	1.000	1.276	0.742	0.564	0.475
0.300	0.105	0.555	0.080	0.017	0.000
	0.263	0.795	0.210	0.071	0.025
	0.421	1.005	0.374	0.178	0.092
	0.579	1.182	0.542	0.322	0.209
	0.737	1.318	0.684	0.463	0.345
	0.895	1.402	0.772	0.557	0.444
	1.000	1.422	0.799	0.593	0.490
0.400	0.105	0.619	0.099	0.025	0.008
	0.263	0.860	0.233	0.083	0.033
	0.421	1.093	0.405	0.195	0.104
	0.579	1.302	0.585	0.345	0.225
	0.737	1.471	0.739	0.493	0.365
	0.895	1.578	0.836	0.592	0.468
	1.000	1.596	0.862	0.627	0.510
0.500	0.105	0.701	0.123	0.036	0.015
	0.263	0.945	0.263	0.098	0.042
	0.421	1.202	0.444	0.215	0.116
	0.579	1.445	0.635	0.372	0.242
	0.737	1.646	0.801	0.526	0.386
	0.895	1.777	0.907	0.630	0.492
	1.000	1.794	0.933	0.664	0.532
0.600	0.105	0.809	0.155	0.051	0.023
	0.263	1.056	0.300	0.116	0.053
	0.421	1.339	0.491	0.240	0.131
	0.579	1.617	0.694	0.402	0.262
	0.737	1.850	0.872	0.563	0.410
	0.895	2.001	0.985	0.671	0.519
	1.000	2.019	1.012	0.704	0.557
0.900	0.105	1.291	0.300	0.115	0.058
	0.263	1.534	0.459	0.192	0.096
	0.421	1.886	0.678	0.335	0.188
	0.579	2.242	0.917	0.520	0.335
	0.737	2.534	1.134	0.709	0.505
	0.895	2.727	1.290	0.851	0.641
	1.000	2.795	1.346	0.906	0.698

NUREG/CR-3723
 ORNL/CSD/TM-216
 Dist. Category RF

Internal Distribution

- | | | | |
|--------|------------------|--------|-------------------------------|
| 1-5. | D. G. Ball | 26. | A. P. Malinauskas |
| 6. | B. R. Bass | 27. | R. K. Nanstad |
| 7. | S. E. Bolt | 28. | D. J. Naus |
| 8. | R. H. Bryan | 29-30. | C. E. Pugh |
| 9. | J. W. Bryson | 31. | G. C. Robinson |
| 10-14. | R. D. Cheverton | 32. | K. R. Thoms |
| 15. | J. M. Corum | 33. | H. E. Trammell |
| 16. | W. R. Corwin | 34. | J. N. Tunstall |
| 17. | J. S. Crowell | 35. | J. D. White |
| 18. | J. B. Drake | 36. | G. E. Whitesides |
| 19. | D. M. Eissenberg | 37-39. | G. D. Whitman |
| 20. | D. S. Griffith | 40. | R. M. Widgeon |
| 21. | R. C. Gwaltney | 41. | ORNL Patent Office |
| 22. | T. L. Hebble | 42. | Central Research Library |
| 23. | S. K. Iskander | 43. | Document Reference Section |
| 24. | J. J. McGowan | 44-45. | Laboratory Records Department |
| 25. | J. G. Merkle | 46. | Laboratory Records (RC) |

External Distribution

47. C. Z. Serpan, Division of Engineering Technology, Nuclear Regulatory Commission, Washington, DC 20555
48. M. Vagins, Division of Engineering Technology, Nuclear Regulatory Commission, Washington, DC 20555
49. Director, Division of Reactor Safety Research, Nuclear Regulatory Commission, Washington, DC 20555
50. Office of Assistant Manager for Energy Research and Development, Department of Energy, Oak Ridge Operations Office, Oak Ridge, TN 37831
- 51-52. Technical Information Center, DOE, Oak Ridge, TN 37831
- 53-327. Given distribution as shown in Category RF (NTIS-10)

NRC FORM 325 (2-84) NRCM 1102 3251 3202		U.S. NUCLEAR REGULATORY COMMISSION		1. REPORT NUMBER (Assigned by TIDC add Vol. No. if any) NUREG/CR-3723 ORNL/CSD/TM-216	
BIBLIOGRAPHIC DATA SHEET					
SEE INSTRUCTIONS ON THE REVERSE					
7. TITLE AND SUBTITLE Stress-Intensity-Factor Influence Coefficients for Surface Flaws in Pressure Vessels				J. LEAVE BLANK	
5. AUTHOR(S) D. G. Ball*, B. R. Bass*, J. W. Bryson, R. D. Cheverton and J. B. Drake*				4. DATE REPORT COMPLETED MONTH: January YEAR: 1985	
7. PERFORMING ORGANIZATION NAME AND MAILING ADDRESS (Include Zip Code) Oak Ridge National Laboratory P. O. Box X Oak Ridge, TN 37830				6. DATE REPORT ISSUED MONTH: February YEAR: 1985	
10. SPONSORING ORGANIZATION NAME AND MAILING ADDRESS (Include Zip Code) Division of Engineering Technology Office of Nuclear Regulatory Research U. S. Nuclear Regulatory Commission Washington, DC 20555				8. PROJECT/TASK/WORK UNIT NUMBER	
12. SUPPLEMENTARY NOTES				9. FIN OR GRANT NUMBER B0119	
13. ABSTRACT (200 words or less) In the fracture-mechanics analysis of reactor pressure vessels, stress-intensity-factor influence coefficients are used in conjunction with superposition techniques to reduce the cost of calculating stress-intensity factors. The present study uses a finite-element code, together with a virtual crack extension technique, to obtain influence coefficients for semielliptical surface flaws in a cylinder, and particular emphasis was placed on mesh convergence (less than 1% error was sought in the results from any one mesh construction parameter). Comparison of the coefficients with those obtained by other investigators shows good agreement. Furthermore, stress-intensity factors obtained by superposition for a severe thermal-transient loading condition agree within 1% of the values calculated by a direct finite-element method. Influence coefficients were calculated for three specific axially oriented semielliptical surface flaws. The first was a 2-m-long inner-surface flaw in a nuclear reactor pressure vessel with depth-to-wall-thickness ratios between 0.2 and 0.9. The second was an inner-surface flaw in the reactor vessel with a surface-length-to-depth ratio of 6 and with depth-to-wall-thickness ratios between 0.05 and 0.2. The third was a 1-m-long flaw on the outer surface of a test vessel with depth-to-wall-thickness ratios between 0.1 and 0.9. For the reactor vessel, separate coefficients were calculated for the cladding on the inner surface and for the base-material region. This allows for an accurate accounting of the effect of thermal stresses in the cladding on the stress-intensity factor for surface flaws that extend through the cladding into the base material.				11a. TYPE OF REPORT	
14. DOCUMENT ANALYSIS -- KEYWORDS/DESCRIPTORS Influence coefficients Superposition techniques Fracture mechanics Pressurized thermal shock				b. PERIOD COVERED (Inclusive Dates)	
15. IDENTIFIERS OPEN ENDED TERMS				15. AVAILABILITY STATEMENT Unlimited	
				16. SECURITY CLASSIFICATION (This page) Unclassified (This report) Unclassified	
				17. NUMBER OF PAGES	
				18. PRICE	

120555078877 1 LANIRE
US NRC
ADM-DIV OF TIDC
POLICY & PUB MGT BR-PDR NUREG
W-501
WASHINGTON DC 20555